ACS Infectious Diseases

Article

Molecular Hybridization-Inspired Optimization of Diarylbenzopyrimidines as HIV-1 Nonnucleoside Reverse Transcriptase Inhibitors with Improved Activity against K103N, E138K Mutants, and Pharmacokinetic Profiles

Sheng Han, Yali Sang, Yan Wu, Yuan Tao, Christophe Pannecouque, Erik De Clercq, Chunlin Zhuang, and Fener Chen

ACS Infect. Dis., **Just Accepted Manuscript** • DOI: 10.1021/acsinfecdis.9b00229 • Publication Date (Web): 10 Oct 2019

Just Accepted

is published by the American Chemical Society. 1155 Sixteenth Street N.W., Washington, DC 20036

Molecular Hybridization-Inspired Optimization of Diarylbenzopyrimidines as HIV-1 Nonnucleoside Reverse Transcriptase Inhibitors with Improved Activity against K103N, E138K Mutants, and Pharmacokinetic Profiles

Sheng Han,[†,‡] Yali Sang,[†,‡] Yan Wu,[†,‡] Yuan Tao,[†,‡] Christophe Pannecouque,[§] Erik De Clercq,[§] Chunlin Zhuang,[,†,‡] and Fen-Er Chen [*,†,‡]*

[†]Engineering Center of Catalysis and Synthesis for Chiral Molecules, Department of Chemistry, Fudan University, Shanghai 200433, People's Republic of China

[‡]Shanghai Engineering Center of Industrial Asymmetric Catalysis for Chiral Drugs, Shanghai 200433, People's Republic of China

[§]Rega Institute for Medical Research, KU Leuven, Herestraat 49, B-3000 Leuven, Belgium

Corresponding Authors: *(F.C.). E-mail: rfchen@fudan.edu.cn.; (C.Z.): zclnathan@163.com.

Molecular hybridization is a powerful strategy in drug discovery. A series of novel diarylbenzopyrimidine (DABP) analogues were developed by the hybridization of FDA-approved drugs etravirine (ETR) and efavirenz (EFV) as potential HIV-1 nonnucleoside reverse transcriptase inhibitors (NNRTIs). Substituent modifications resulted in the identification of new DABPs with the combination of the strengths of the two drugs, especially compound **12d,** which showed promising activity toward the EFV-resistant K103N mutant. **12d** also had a favorable pharmacokinetic (PK) profile with liver microsome clearances of 14.4 μL/min/mg (human) and 33.2 μL/min/mg (rat) and an oral bioavailability of 15.5% in rat. However, its activity against the E138K mutant was still unsatisfactory; E138K is the most prevalent NNRTI resistance-associated mutant in ETR treatment. Further optimizations resulted in a highly potent compound (**12z**) with no substituents on the phenyl ring and a 2-methyl-6-nitro substitution pattern on the 4-cyanovinyl-2,6-disubstitued phenyl motif. The antiviral activity of this compound was much higher than those of ETR and EFV against the WT, E138K and K103N variants (EC_{50} = 3.4, 4.3 and 3.6 nM, respectively), and the cytotoxicity was decreased while the selectivity index (SI) was increased. In particular, this compound exhibited acceptable intrinsic liver microsome stability (human, 34.5 μL/min/mg; rat, 33.2 μL/min/mg) and maintained the good PK profile of its parent compound EFV and showed an oral bioavailability of 16.5% in rat. Molecular docking and structure−activity relationship (SAR) analysis provided further insights into the binding of the DABPs with HIV-1 reverse transcriptase and provided a deeper understanding of the key structural features responsible for their interactions.

Keywords: Molecular Hybridization; Diarylbenzopyrimidines; HIV-1; Reverse Transcriptase; NNRTI; PK

According to the 2017-WHO report, approximately 36.9 million people were infected with human immunodeficiency virus (HIV) worldwide, 1.8 million people were newly infected with HIV, and 0.94 million people died.[1] Acquired immune deficiency syndrome (AIDS), one of the most devastating infectious diseases that has not been eradicated, still requires potent antiretroviral therapy agents to reduce the death toll related to human immunodeficiency virus type 1 (HIV-1), the etiological agent of AIDS.

Currently, therapies against AIDS are based on several classes of anti-HIV drugs that target different steps of the viral life cycle:[2] fusion inhibitors (FIs), the coreceptor antagonist (maraviroc), integrase strand transfer inhibitors (INSTIs), protease inhibitors (PIs), and nucleoside and nonnucleotide reverse transcriptase inhibitors (NRTIs and NNRTIs). NNRTIs are key drugs in highly active antiretroviral therapy (HAART).[3] However, the effectiveness of NNRTIs has been significantly reduced because of the rapid development of resistance in a growing number of mutant viral strains.[4-7] Efavirenz (EFV, **1**) is an early generation NNRTI. In the Gilead 934 study, 84% of EFV resistance possessed the K103N mutation.[8] It is reported to be ineffective against the K103N variant.[9-11] Therefore, the K103N was the most prevalent NNRTI resistance-associated mutation (RAM) in EFV treatments.[12-14]

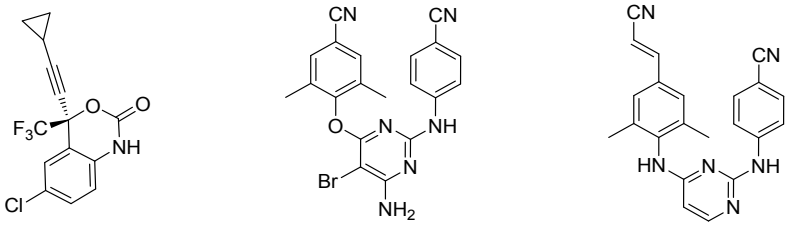

1 (Efavirenz) **2 (Etravirine)** **3 (Rilpivirne)**

Figure 1. The chemical structures of efavirenz, etravirine and rilpivirine

Diarylpyrimidine (DAPY) analogues are one of the most potent families of NNRTIs developed thus far. Etravirine (ETR, **2**) and rilpivirine (RPV, **3**), representative DAPYs approved by the FDA, exhibit high anti-viral activity against wild-type (WT) and the K103N mutation.[15] This phenomenon may be caused by the fact that DAPY inhibitors bind to the nonnucleoside reverse transcriptase inhibitor binding pocket (NNIBP) to form a flexible "horseshoe" conformation, minimizing the loss of binding stabilization.[16-19] However, E138K, the most prevalent NNRTI RAM, is recognized to be the reason for the failure of RPV or ETR treatments.[20-26] About 77% patients failed with RPV treatments due to the E138K mutation (NCT00543725).[12] Besides, the oral

bioavailability or PK properties is another important aspect to limit the efficacy of NNRTIs.[27-29] The absolute oral bioavailability of ETR in human is still unknown probably due to its bad solubility and lack of an intravenous formulation.[30-32] Thus, finding novel NNRTIs to overcome drug resistance and improved PK profiles is of great importance.

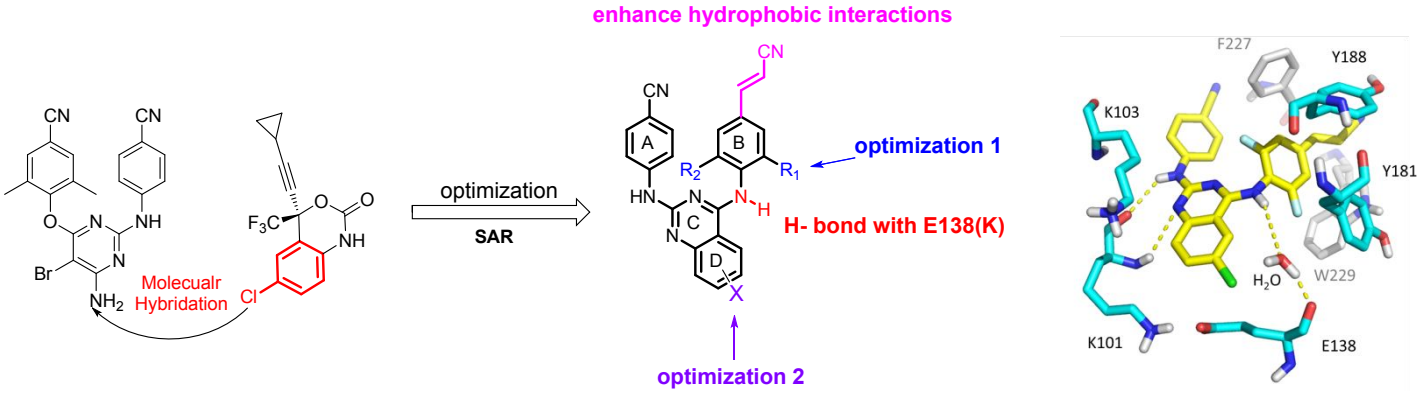

Figure 2. The optimization strategy of DABPs

In our previous work, we reported that several DABP hybrids based on ETR and DPC083 showed promising HIV-1 inhibitory activities with low cytotoxicities and high selectivity indexes (SI).[33] In this study, we used a molecular hybridization strategy on the basis of ETR and EFV to address the drawbacks of two generations of NNRTIs, improve the potency of DABPs against the K103N and E138K mutants, expand the SARs and improve the PK profiles. These structural optimizations focused on three important factors. (1) Conversion of the ether linkage between rings B and C to an amino group to allow the formation of additional water-mediated hydrogen bonds with the carbonyl of E138. (2) Insertion of a vinyl group between the cyano group and ring B to extend the π–π stacking interactions with the highly conserved amino acid W229 around the hydrophobic tunnel in RT. (3) Various substituents with different sizes and electronic properties were introduced on ring B and ring D.

RESULTS AND DISCUSSION

Chemistry

The synthetic route to the desired quinazoline diamines is outlined in Scheme 1. Briefly, the first set of key intermediates (**6a-f**) were synthesized via a well-established two-step procedure.[34-38] In the meantime, *ortho*-nitro benzoic acids **7a-f** were catalytically hydrogenated to obtain anthranilic acids **8a-f**, which were subsequently

treated with urea to afford quinazolinediones **9a-f**.[33, 39] **9a-f** were then reacted with phosphorus oxychloride in the presence of *N,N*-diisopropylethylamine, leading to the formation of 2,4-dichloroquinazolines **10a-f**.[40] Without purification, key intermediates (**10a-f**) were immediately reacted with aromatic amines **6a-f** under Pd catalysis[38, 41, 42] to yield 4-substituted-2-chloroquinazolines **11a-z**.[43-47] Finally, **11a-z** were reacted with 4-aminobenzonitriles to give target quinazoline diamines **12a-z**.[48]

Scheme 1. Synthesis of quinazoline diamines 12a-z

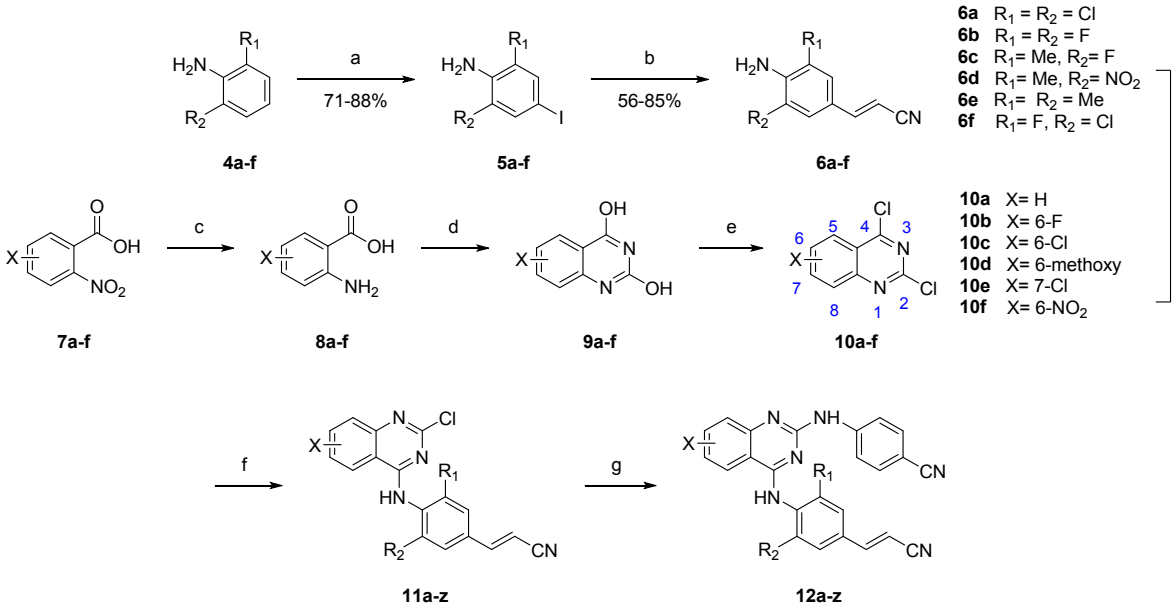

Reagents and conditions: (a) $NaHCO_3$, iodine chloride, methanol, dichloromethane, room temperature, 6 h; (b) acrylonitrile, 10% Pd/C wet, P(o-Tol)$_3$, sodium acetate, tetrabutylammonium bromide, *N,N*-dimethylacetamide, 140 ^oC, 12 h; (c) 10% Pd/C wet, hydrogen atmosphere (balloon), ethanol, reflux, 24 h; (d) urea, 180 ^oC, 3 h; (e) $POCl_3$, *N,N*-diisopropylethylamine, reflux, 6 h; (f) (*E*)-3-(4-amino-3,5-disubstituted)acrylonitrile, palladium acetate, DavePhos, K_3PO_4, *N,N*-dimethylacetamide, 140 ^oC, 12 h; (g) 4-aminobenzonitrile, *n*-butanol, reflux, 6-8 h.

Molecular hybridization of ETR and EFV leads to promising antiviral activity with a good combination of their strengths.

Based on the modeling study, the chlorophenyl group of EFV was introduced as ring D by molecular hybridization (Figure 2). Four novel 6-chloride quinazoline diamines (**12a-d**) with different substituents on ring B were synthesized. They maintained the activities of the parent compounds (EFV and ETR) against WT HIV-1. The activity of compound **12a** against K103N was ~5-fold greater than that of EFV. Next, we replaced the chloride on ring B with a fluoride, as it might improve the potency and other properties, such as conformational restriction, lipophilicity and metabolic stability.[49] Compound **12b**, with two fluoride substituents on ring B, showed the best antiviral potency against WT HIV and moderate cytotoxicity, but it was not the most active compound in this series against the K103N mutant strain. Replacement of one fluoride with a methyl group, which should improve the conformation, on ring B (compound **12c**) significantly improved activity against the K103N mutant virus, and the activities against WT HIV and the E138K were maintained. Then, a nitro group was introduced as it is considered to be a versatile and unique functional group with various therapeutic effects.[50-52] When compared with **12c** and EFV, compound **12d** had similar potencies against WT HIV, the E138K and K103N mutants.

Table 1. Activity of **12a-d** against HIV-1 III_B, E138K, K103N strains and cytotoxicity in MT-4 cells.[a]

Compound	X	R_1	R_2	EC_{50}[b] (nM)			CC_{50}[c] (nM)	SI[d]
				HIV-1 III_B	E138K	K103N		III_B
12a	6-Cl	-Cl	-Cl	13.6 ± 9.1	41.6 ± 16.8	29.4 ± 0.2	5264 ± 1348	390
12b	6-Cl	-F	-F	9.6 ± 2.8	13.1 ± 0.2	42.3 ± 10.5	12435 ± 5079	1301
12c	6-Cl	$-CH_3$	-F	10.3 ± 3.1	11 ± 0.2	12.1 ± 3.5	9200 ± 1514	890
12d	6-Cl	$-CH_3$	$-NO_2$	10.6 ± 10.0	17.7 ± 2.7	10.2 ± 0.8	3954 ± 1154	375
ETR				3.9 ± 1.4	10.9 ± 7.4	3.5 ± 0.9	>4620	>1165
EFV				3.2 ± 1.4	5.4 ± 1.3	147.4 ± 85.9	> 40196	>2000
RPV[e]				1	6	1	>3980	3989

[a]All data represent the mean values for at least three independent experiments.

[b]EC_{50}: The effective concentration required to protect MT-4 cells against virus-induced cytopathicity by 50%.

[c]CC_{50}: The cytotoxic concentration of the compound that reduces the normal uninfected MT-4 cell viability by 50%.

[d]SI: selectivity index, ratio of CC_{50}/EC_{50} (WT).

[e]The data were obtained from the same laboratory (Prof. Erik De Clercq, Rega Institute for Medical Research, KU Leuven, Belgium) with the same method.[53]

Table 2. Rat PK profile and liver microsome stability of **12d** [a]

Liver microsome stability		Rat PK profile			
		Parameter	5.0 mg/kg (p.o.)	10.0 mg/kg (p.o.)	1.0 mg/kg (i.v.)
the clearance rate of rat (μL/min/mg)	30.6	AUC_{all} (ng*h/mL)	756 ± 129	1183 ± 75	983 ± 131
		AUC_{inf} (ng*h/mL)	768 ± 129	1198 ± 71	991 ± 131
		MRT_{inf} (h)	6.61 ± 0.70	7.45 ± 1.78	3.10 ± 0.21
		$t_{1/2}$ (h)	3.95 ± 1.00	3.15 ± 0.40	4.02 ± 0.37
the clearance rate of human (μL/min/mg)	14.4	T_{max} (h)	1.0 ± 0.0	1.33 ± 0.58	—
		C_{max} (ng/mL)	128 ± 74	133 ± 100	—
		F (%)	15.5 ± 2.6	12.1 ± 0.7	—

[a]PK parameters (mean ± SD, n = 3).

Next, we examined the drug-like properties of the new DABP hybrids, and compound **12d** was selected for its promising antiviral potency against both WT and mutant strains. The liver microsome stability and rat PK profile of compound **12d** were examined. The intrinsic rat and human microsome clearances of **12d** were 30.6 and 14.4 μL/min/mg proteins, respectively (Table 2), showing the property of moderate clearance (classification: human, low < 8.6 μL/min/mg, high > 47.0 μL/min/mg; rat, low < 13.2 μL/min/mg, high > 71.9 μL/min/mg).[54] The PK results showed that compound **12d** was absorbed with short T_{max} values (1 h and 1.33 h), favorable half-lives (3.95 h and 3.15 h), and mean residence times (MRTs) of 6.61 h and 7.45 h when orally administered at two doses of 5 mg/kg and 10 mg/kg, respectively. The C_{max} values were 128 and 133 ng/mL. Moreover, the oral bioavailabilities (F) were calculated to be acceptable values of 15.5% and 12.1%, respectively, which were comparable to that of EFV (16%).[55] A single-dose toxicity test of compound **12d** was carried out in rats. After

intragastric administration of **12d** at a dose of 183 mg/kg body weight, no mortality was observed in the rats, and there were no abnormal body weight decreases in the animals in the week following administration.

Further optimizations indicate an SAR of DABP hybrids and provide derivatives with much higher antiviral activities against WT, E138K and K103N variants and improved PK.

Encouraged by the results of 6-chloride hybrids **12a-d**, we further replaced the chloride with different functional groups (e.g., fluorine, methoxy, hydroxy, and nitro groups) to establish the SAR of the DABP hybrids. This region of E138 was tolerant of substitutions, and these distinct substitution patterns could potentially affect the mutant variant (Figure 2).

First, 6-fluorine quinazoline diamines **12e-i** were synthesized. They showed significantly improved potencies against the E138K and K103N mutant strains when compared with their corresponding chlorinated analogues (**12a-d**). Compound **12f** had better or comparable activities against WT HIV-1, E138K and K103N mutant strains (EC_{50} = 4.6, 4.6, and 5.0 nM, respectively) relative to those of ETR and EFV, and it showed a high SI value (SI = 3924).

In addition to fluorine and chlorine, electron-donating groups (e.g., methoxy and hydroxy groups) were introduced to afford compounds **12j-l**. Unfortunately, although the cytotoxicity was much lower, this series showed decreased activities toward the WT HIV-1, E138K and K103N mutant strains. Then, the nitro group was similarly introduced at the C6 position of ring D, affording compound **12n**. Compound **12n** showed a 2-fold decrease in activity against the HIV-1 WT strain (EC_{50} = 9.6 nM) compared with its corresponding 6-fluorinated analogue **12g** (EC_{50} = 5.3 nM), and its activity was comparable to that of its corresponding 6-chloride analogue **12b** (EC_{50} = 9.6 nM). Remarkably, the activity of **12n** against the E138K mutant strain was greater (EC_{50} value of 5.8 nM) than those of **12b** (EC_{50} = 13.1 nM) and ETR (EC_{50} = 10.9 nM). Moreover, introducing a nitro group into a drug molecule should be careful due to associated toxicity issues.[50] Surprisingly, the cytotoxicity of **12n** was determined, and it showed the highest CC_{50} and SI values (CC_{50} >216 μM, SI= 22498) of all compound in this series. Compound **12n** showed moderate activity against the K103N mutant strain, and its EC_{50} was higher than that of EFV.

Table 3. Activity of **12e-z** against HIV-1 III_B, E138K, K103N strains and cytotoxicity in MT-4 cells.[a]

Compound	X	R_1	R_2	EC_{50}[b] (nM)			CC_{50}[c] (nM)	SI[d]
				HIV-1 III_B	E138K	K103N		III_B
12e	6-F	-Cl	-Cl	8.4 ± 9.2	17.9 ± 2.1	10.1 ± 2.3	3373 ± 1394	405
12f	6-F	-F	-Cl	4.6 ± 4.6	4.6 ± 1.3	5.0 ± 0.2	17623 ± 1757	3924
12g	6-F	-F	-F	5.0 ± 0.9	5.3	29.6 ± 4.1	8407 ± 1532	1730
12h	6-F	$-CH_3$	-F	3.9 ± 1.1	8.7 ± 0.2	9.8 ± 0.9	7574 ± 1265	1909
12i	6-F	$-CH_3$	$-NO_2$	2.6 ± 0.6	6.0 ± 1.5	4.7 ± 0.2	5070 ± 1036	1925
12j	6-OCH_3	$-CH_3$	$-CH_3$	10.5 ± 6.0	28.0 ± 12.5	11.0 ± 0.7	94347 ± 58197	9000
12k	6-OCH_3	-Cl	-Cl	19.1 ± 14.1	10.0 ± 4.3	27.9 ± 5.1	7319 ± 1066	383
12l	6-OCH_3	-F	-F	9.0 ± 4.6	19.6 ± 10.3	24.6 ± 12.5	12273 ± 6598	1355
12m	6-OH	-F	-F	161 ± 108	76.0 ± 5.9	131.4 ± 2.5	>283750	>1763
12n	6-NO_2	-F	-F	9.6± 3.6	5.8 ± 1.5	38.8 ± 14.9	216838 ± 39782	22498
12o	7-Cl	-Cl	-Cl	8.7 ± 3.7	14.2 ± 2.6	11.2 ± 1.0	4009 ± 757	456
12p	7-Cl	-F	-Cl	11.8 ± 8.2	10.3 ± 2.3	7.8 ± 1.3	52920 ± 20792	4520
12q	7-Cl	-F	-F	7.8 ± 2.8	6.1 ± 0.2	7.2 ± 2.2	144257 ± 65189	18510
12r	7-Cl	$-CH_3$	-F	9.9 ± 5.9	12.1 ± 0.2	9.2 ± 0.9	9108 ± 1100	920
12s	7-Cl	$-CH_3$	$-NO_2$	5.0 ± 3.1	15.6 ± 5.2	19.6 ± 3.7	9227 ± 2762	1888
12t	7-Cl	$-CH_3$	$-NH_2$	15.9 ± 5.5	32.7 ± 2.4	45.5 ± 4.0	9105 ± 1348	569
12u	-H	$-CH_3$	$-CH_3$	10.3 ± 4.1	24.7 ± 13.7	10.8 ± 1.7	25238 ± 9163	2457
12v	-H	-Cl	-Cl	3.7± 0.9	6.6 ± 0.9	4.6 ± 0.2	6436 ± 2729	1781
12w	-H	-F	-Cl	2.5 ± 1.1	4.8 ± 1.1	5.2 ± 0.2	7918 ± 1332	3100
12x	-H	-F	-F	4.7 ± 1.7	8.7 ± 8.3	11.3 ± 1.9	9891 ± 3932	2096
12y	-H	$-CH_3$	-F	10.5 ± 5.5	7.1 ± 1.0	5.0 ± 0.5	6854 ± 488	657
12z	-H	$-CH_3$	$-NO_2$	3.4 ± 0.9	4.3 ± 1.3	3.6 ± 0.9	6138 ± 1897	1827
ETR				3.9 ± 1.4	10.9 ± 7.4	3.5 ± 0.9	>4620	>1165
EFV				3.2 ± 1.4	5.4 ± 1.3	147.4 ± 85.9	> 40196	>2000
RPV				1	6	1	>3980	3989

[a]All data represent the mean values for at least three independent experiments.

[b]EC_{50}: The effective concentration required to protect MT-4 cells against virus-induced cytopathicity by 50%.

[c]CC_{50}: The cytotoxic concentration of the compound that reduces the normal uninfected MT-4 cell viability by 50%.

[d]SI: selectivity index, ratio of CC_{50}/EC_{50} (WT).

Third, moving the chloride to the C7 position placed it still close to residue E138, and the pocket might be tolerant of an additional substituent (Figure 2). On the basis of the results of the 6-substituted analogues, an electron-withdrawing chloride was introduced at the C7 position, yielding compounds **12o-s**. In addition to good potency against WT HIV-1, all compounds in this series exhibited low nanomolar potencies against E138K and K103N mutant strains (EC_{50} values ranging from 6.1 to 15.6 nM and 7.2 to 19.6 nM, respectively). Remarkably, compound **12q** showed better or comparable activity (EC_{50}= 6.1 and 7.2 nM, respectively) against the E138K and K103N mutant strains relative to those of ETR and EFV as well as high CC_{50} (=144 μM) and SI (18510) values. The reduction of the nitro group of **12s** afforded compound **12t**, which showed 2 to 3-fold lower potency against the WT, E138K and K103N mutant strains.

Finally, we removed the substituent on ring D to further elucidate the SAR. Compounds **12u-z** were synthesized on the basis of representative substituents on ring D in the **12a-t** series. Fortunately, all the compounds exhibited excellent potency against WT HIV-1 (EC_{50} = 2.5–10.5 nM), the E138K mutant strain (EC_{50} = 4.3–8.7 nM) and the K103N mutant strain (EC_{50} = 3.6–11.3 nM), except for **12u**. Compound **12u**, with a 2,6-dimethyl substitution pattern, had activity comparable to those of corresponding compound **12j** against WT, E138K and K103N mutant strains (EC_{50} = 10.3 nM, 24.7 and 10.8 nM, respectively). When changing the chloride or fluoride at the *ortho* position of ring B (**12v-y**), the activity was improved, and activities better than or comparable to those of the drugs ETR or EFV against E138K and K103N were observed. Considering the promising activities of **12i**, **12n** and **12s**, the 2-methyl-6-fluoro motif was then replaced by a 2-methyl-6-nitro pattern on ring B to afford compound **12z**. This compound showed a great combination of the strength of the two drugs (ETR and EFV). Compound **12z** was 2.5-fold more potent than ETR against E138K and was 41-fold more potent than EFV against K103N. The EC_{50} value of **12z** against WT HIV-1 was 3.4 nM relative to 3.9 nM for ETR and 3.2 nM for EFV.

As they showed the best anti-E138K and K103N activities, compounds **12d**, **12f**, **12n**, **12q**, **12w** and **12z** were selected for further evaluation against the HIV-1 mutant RT enzyme (Table 4). They exhibited activities

better or comparable to those of ETR and EFV at the enzymatic level, with IC_{50} values of 7.0 to 18.1 nM, showing a good correlation (R^2 = 0.95) with their antiviral activities in MT-4 cells (Figure S2). The time-of-addition experiment was also performed to support that RT is the main and exclusive target of these compounds. [56] The results clearly indicated our compounds acting as the NNRTI-type mode of action and better than the reference compounds NVP and ETR (Figure S3).

Table 4. The activity of selected compounds against WT HIV-1 RT enzyme.[a]

Compound	12d	12f	12n	12q	12w	12z	ETR	EFV
IC_{50} (nM)	17.7 ± 0.8	11.3 ± 0	18.1 ± 0.9	12.4 ± 1.5	7.0 ± 0.3	13.7 ± 1.6	11 ± 0	12.7 ± 9.5

[a]IC_{50}: inhibitory concentration of test compound required to inhibit WT HIV-1 RT polymerase activity by 50%.

Compounds **12n** and **12z** were then selected for PK studies based on their structural features (containing a nitro group), marked antiviral activities against WT and mutant strains, and/or high SI. Unfortunately, the oral bioavailability (F) of compound **12n** was calculated to be ~ 2% at 5 mg/kg (see the Supporting Information Table S1). This result may be attributable to the nitro group at the 6-position of the quinazoline core exhibiting an electron-withdrawing effect and making the π-electron system more electron deficient, leading to its metabolic instability[57] and poor bioavailability. Fortunately, the oral bioavailability (F) of **12z**, with no substituents on ring D, was significantly improved to 16.5% at a dose of 5 mg/kg in rats. The intrinsic rat and human microsome clearances of **12z** were 33.2 and 34.5 μL/min/mg proteins, respectively (Table 5). The PK study and safety assessment of **12z** showed that it was absorbed with mean residence times (MRTs) of 11.8 h and 11.4 h at these two doses. The C_{max} of **12z** was 39.9 ng/mL at a dose of 5 mg/kg. A single-dose toxicity test of compound **12z** in rats showed no mortality, and there was no abnormal body weight decrease in the animals in the week following an intragastrical dose at 293 mg/kg body weight (Figure S1). The above results indicate that compound **12z** could be an orally bioavailable candidate for treating human HIV-1 infection.

Table 5. Rat PK profile and liver microsome stability of **12z** [a]

Liver microsome stability		Rat PK profile		
		Parameter	5.0 mg/kg (p.o.)	1.0 mg/kg (i.v.)
the clearance rate of rat (μL/min/mg)	33.2	AUC_{all} (ng*h/mL)	39.9 ± 12.5	48.4 ± 9.8
		AUC_{inf} (ng*h/mL)	—	50.4 ± 9.7
		MRT_{inf} (h)	11.8 ± 4.7	0.65 ± 0.15
the clearance rate of human (μL/min/mg)	34.5	$t_{1/2}$ (h)	—	3.26 ± 1.37
		T_{max} (h)	13.3 ± 11.0	—
		C_{max} (ng/mL)	4.16 ± 0.31	—
		F (%)	16.5 ± 5.2	—

[a]PK parameters (mean ± SD, n = 3).

Molecular modeling analysis provides further insights into the binding of the DABPs to HIV-1 RT.

Compounds **12d**, **12n** and **12z** were selected for the molecular modeling study to predict their binding modes with RT and further clarify their activities. The E138K or K103N mutated enzyme was generated and its energy was minimized using BioLuminate. The docking study was performed by Glide package using default parameters. After docking study, Desmond molecular dynamics simulations was run using the docking poses with the best Glidescore. The predicted results were then selected after 3 ns simulations with a suitable RMSD (~3 Å, see supporting information). They showed several common features (Figure 3). (1) Consistent with previous publications,[58] the NH linkage of ring B and C formed a water-mediated hydrogen bonding interaction with the carbonyl of E138. (2) The cyanovinyl group enhanced the interactions with Y181, Y188, F227, and W229 in the modified hydrophobic tunnel.[58] (3) The NH linker connecting the central pyridine ring and the cyano-phenyl ring and the nitrogen of the pyrimidine formed hydrogen bonds with the backbone of K101.[59, 60] The distance between the 6-chloride substituent of compound **12d** and E138/K138 was very short (Figure 3A, 3D and 3G). Compound **12n**, with a 6-nitro group, formed an additional water-mediated hydrogen bond with the carbonyl of E138 (Figure 3B). The orientation of the new K138 was different due to the existence of the adjacent K101, making the space between the residue and ring D more tolerated than it was in WT RT (Figure 3D, 3E and 3F). The water-mediated

hydrogen bond was still observed in the mutant strain. The binding mode of **12n** with RT explained its higher activity against the E138K mutant than against the WT strain. Compound **12z** had a binding mode similar to that of **12n** (Figure 3C and 3F). The 2-methyl-6-nitro and 2,6-difluro groups restricted the conformation of ring B, making it more orientated to the new N103, thus resulting in a water-mediated hydrogen bond with the NH of amide (the distance between nitro/ fluorine and hydrogen was 4-5 Å, Figure 3G, 3H and 3I).

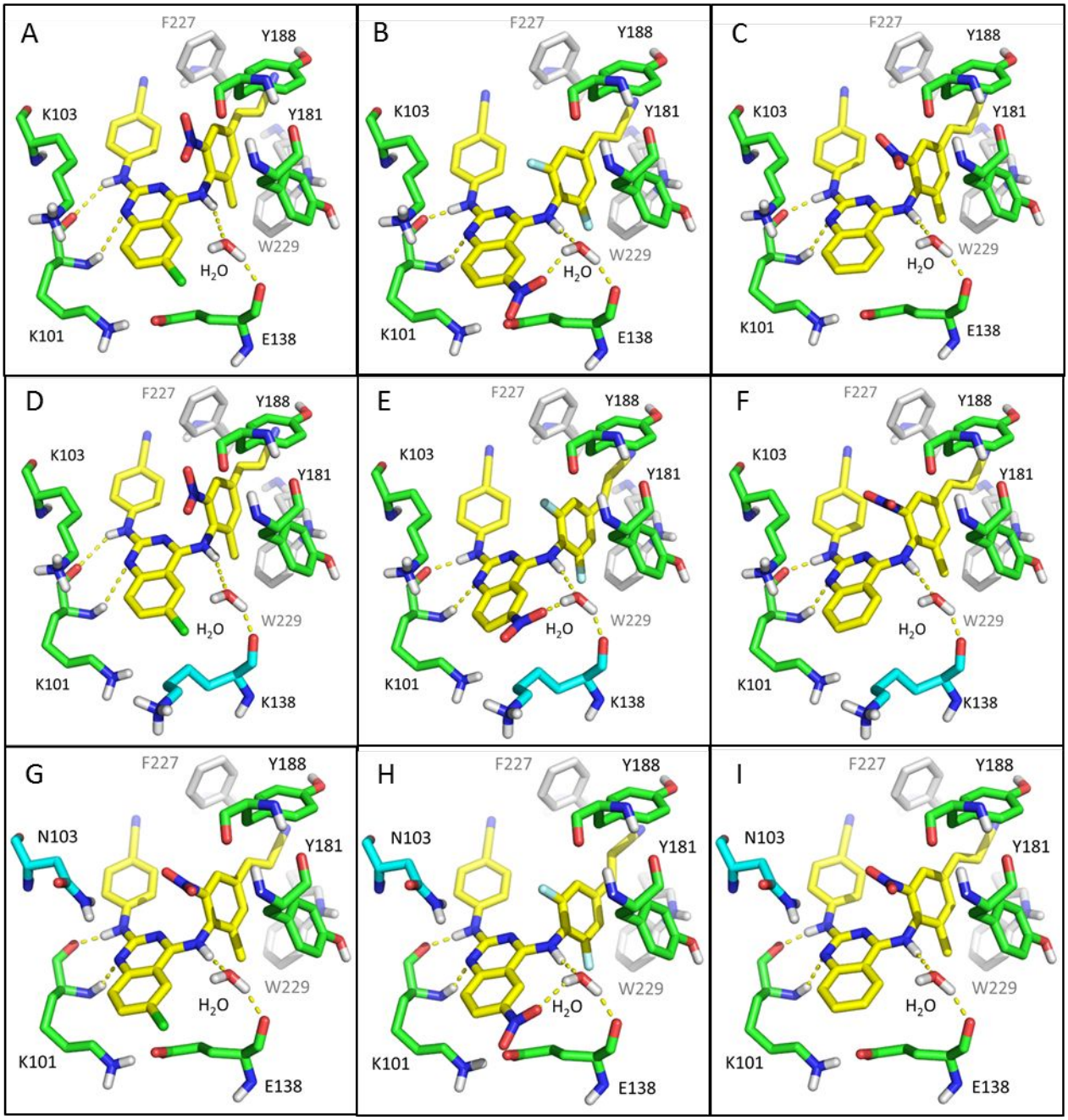

Figure 3 Predicted binding modes of **12d**, **12n** and **12z** with the HIV-1 WT and E138K mutant RT crystal structure. (A) WT with **12d** (yellow); (B) WT with **12n** (yellow); (C) WT with **12z** (yellow); (D) E138K mutant RT with **12d**; (E) E138K mutant RT with **12n**; (F) E138K mutant RT with **12z**; (G) K103N mutant RT with **12d**;

(H) K103N mutant RT with **12n**; (I) K103N mutant RT with **12z**. The carbons of the compounds are depicted in yellow. Residues involved in interactions are shown as green or gray sticks. Mutated residues are depicted as cyan sticks. Hydrogen bonds are depicted as yellow dashed lines.

Conclusion

A series of novel quinazoline-2,4-diamine derivatives were designed by molecular hybridization and synthesized. SAR studies led to the discovery of a number of HIV-1 inhibitors with nanomolar potencies that addressed the drawbacks of ETR and EFV against two of the most prevalent NNRTI RAMs and PK profiles. The results of biological evaluations highlight the promise of DABP compounds as potential drug candidates. (1) The new DABPs represent a novel class of NNRTI showing potent inhibition of the HIV-1 WT strain (HIV-1 III_B) not only in cells but also with the free RT enzyme. (2) They are also active against HIV-1 E138K and K103N mutants in the low nanomolar concentration range, acceptable SI values and low cytotoxicities as compared to ETR and EFV. (3) Molecular modeling studies provided further insights into the allosteric binding of DABPs to HIV-1 WT and mutant RT. (4) They possess acceptable metabolic stabilities and good oral bioavailability for the eventual clinical treatment of human HIV-1 infection. The best compound **12z** exhibited EC_{50} values of 3.4, 4.3 and 3.6 nM against the WT, E138K and K103N variants, had acceptable intrinsic liver microsome stability (human, 34.5 μL/min/mg; rat, 33.2 μL/min/mg), and showed an oral bioavailability of 16.5% in rat. The compound could be a potential lead for further optimization in anti-RT drug discovery.

Experimental section

1. Chemistry

Chemical reagents and solvents, purchased from commercial sources, were of analytical grade and used without further purification. All air-sensitive reactions were under a nitrogen atmosphere. All the reactions were monitored by TLC on the pre-coated silica gel G plates at 254 nm under a UV lamp using ethyl acetate/*n*-hexane as the eluent. Column chromatography was performed on glass column packed with silica gel (200-300 mesh) using ethyl acetate/*n*-hexane as the eluent. Melting points were measured on a SGW X-1 microscopic melting point apparatus. ^{1}H NMR and ^{13}C NMR spectra were recorded on a Bruker AV400 MHz spectrometer in DMSO-d_6. Chemical shifts were reported in δ (ppm) units relative to the internal standard tetramethylsilane (TMS). Mass spectra and HRMS were obtained on a Waters Quattro Micromass instrument and Brukersolari X-70 FT-MS instrument, respectively, using electrospray ionization (ESI) techniques. The purities of the target compounds were ≥ 95%, measured by LC-MS, performed on an Waters 2695 system with UV detector and Synergi 4 μm Hydro-RP 80 Å column (250×4.6 mm), eluting with a mixture of water (A) and methanol (B) (V_A:V_B=50:50 to 10:90) over 30 min with a flow rate of 1.0 mL/min and detection at 254 nm.

*1.1 General procedure to prepare the intermediates of **6a-f**:*

A mixture of various kinds of aniline (50 mmol, 1.0 eq), sodium bicarbonate (12.6 g, 150 mmol, 3.0 eq) and methanol (70 mL) was stirred at room temperature. A solution of iodine chloride (8.93 g, 55 mmol, 1.1 eq) in dichloromethane (70 mL) was added to the mixture dropwise in 20 minutes, then the solution was stirred at room temperature for 6 h until GC-MS showed that the reaction was completed. The resulting mixture was filtered, then the filtrate was concentrated. The residue was diluted with ethyl acetate, washed with an aqueous sodium thiosulfate solution, dried with anhydrous sodium sulfate, filtered and concentrated to afford the crude **5a-f**. The crude product was used in the next step without further purification.

The crude **5a-f** (50 mmol, 1.0 eq), acrylonitrile (5.30 g, 100 mmol, 2.0 eq)， P(o-tol)$_3$ (1.52 g, 5 mmol, 0.1 eq), tetrabutylammonium bromide (16.1 g, 50 mmol, 1.0 eq), 10% Pd/C wet (2.7 g, 0.05 eq), sodium acetate (4.93 g, 60 mmol, 1.2 eq) and *N, N*-dimethylacetamide (200 mL) was heated at 140 °C under nitrogen atmosphere for 12 h until GC-MS showed the reaction was completed. The resulting mixture was filtered, diluted with ethyl acetate

and washed with brine. Then, it was dried over anhydrous sodium sulfate, concentrated and purified by chromatography to obtain a white or pale yellow solid **6a-f** of 42-75% yield in two steps.

*1.2 General procedure to prepare the intermediates of **9a-f**:*

Commercially available 2-nitrobenzoic acid **7a-f** (177 mmol, 1.0 eq), 10% wet Pd/C (1.5 g, 0.05 eq) and ethanol (300 mL) were refluxed under the atmosphere of hydrogen balloon reduction for 24 h. After TLC showed the reaction was completed, the result mixture was filtered and concentrated to afford the crude reduction product **8a-f**.

A flask containing substituted anthranilic acids **8a-f** (177 mmol, 1.0 eq) and urea (159 g, 2.65 mol, 15.0 eq) was heated at 180 °C. After 3 h, the reaction mixture was cooled to 100 °C and an equal volume of water was added. The obtained suspension was left to stir for another 30 min, after which it was cooled to room temperature. The precipitate was filtered, washed with fresh water and dried in vacuum. Quinazoline-2,4-diones **9a-f** were white or pale yellow solids of 55-78% yield in two steps.

*1.3 General procedure to prepare the intermediates of **11a~z**:*

Quinazoline-2,4-diones **9a-f** (13 mmol, 1.0 eq), *N,N*-diisopropylethylamine (3.37 g, 26 mmol, 2.0 eq) and phosphorus oxychloride (19.9 g, 130 mmol, 10 eq) were refluxed for 6 h to form 2,4-dichloroquinazolines. The cooling mixtures were poured into ice-water before being stirred at room temperature. The resulting precipitates were filtered, washed with fresh cold water and dried in vacuum to give products **10a-f**, which were hygroscopic and unstable in air and were used immediately.

(*E*)-3-(4-amino-3,5-disubstituted)acrylonitrile (**6b-e**, 10 mmol, 1.0 eq), the crude 2,4-dichloroquinazoline **10a-f** (13 mmol, 1.3 eq), palladium acetate (112 mg, 0.5 mmol, 0.05 eq), DavePhos (394 mg, 1 mmol, 0.1 eq), K_3PO_4 (6.37 g, 30 mmol, 3.0 eq) in *N,N*-dimethylacetamide (80 mL) were heated at 140 °C for 12 h under nitrogen atmosphere. 4-Substituted-2-chloroquinazoline was purified by chromatography to obtain a white or pale yellow solid (**11b~d**, **11g~j**, **11l~n**, **11q~u**, **11u** and **11x~z**) of 21-43% yield in two steps.

(*E*)-3-(4-amino-3,5-disubstituted)acrylonitrile (**6a** and **6f**, 10 mmol, 1.0 eq), the crude 2,4-dichloroquinazoline **10a-f** (13 mmol, 1.3 eq), K_3PO_4 (6.37 g, 30 mmol, 3.0 eq) in *N,N*-dimethylacetamide (80 mL) were heated at 140

°C for 12 h under nitrogen atmosphere. The 4-substituted-2-chloroquinazoline was purified by chromatography to obtain a white or pale yellow solid (**11a**, **11e~f**, **11k**, **11o~p**, and **11v~w**) of 15-30% yield in two steps.

*1.4 General procedure to prepare **12a~z**:*

4-Substituted-2-chloroquinazoline **11a~z** (2 mmol, 1.0 eq), 4-aminobenzonitrile (4 mmol, 472 mg, 2.0 eq) in *n*-butanol (5 mL) were refluxed for 6-8 h. The resulting precipitate was filtered off, washed with dichloromethane (5 mL ×3) and dried in vacuum to obtain **12a~z** as a white or pale yellow solid of 37-55% yield.

*1.5 2,6-difluoro-4-iodoaniline (**5b**).* Synthesized following general procedure 1.1. Yield 83%, black solid. ^{1}H NMR (400 MHz, $CDCl_3$) δ 7.21 – 7.08 (m, 2H, Ar*H*), 3.76 (s, 2H, NH_2).

*1.6 2-fluoro-4-iodo-6-methylaniline (**5c**).* Synthesized following general procedure 1.1. Yield 71%, black solid. ^{1}H NMR (400 MHz, $CDCl_3$) δ 7.20 – 7.14 (m, 2H, Ar*H*), 3.66 (s, 2H, NH_2), 2.14 (s, 3H, CH_3).

*1.7 4-iodo-2,6-dimethylaniline (**5e**).* Synthesized following general procedure 1.1. Yield 88%, black solid. ^{1}H NMR (400 MHz, $CDCl_3$) δ 7.24 (s, 2H, Ar*H*), 3.57 (s, 2H, NH_2), 2.13 (s, 6H, CH_3×2).

*1.8 (E)-3-(4-amino-3,5-dichlorophenyl)acrylonitrile (**6a**).* Synthesized following general procedure 1.1. Yield 56%, white solid. ^{1}H NMR (400 MHz, DMSO-d_6) δ 7.62 (s, 2H, Ar*H*), 7.42 (d, J = 16.6 Hz, 1H, olefinic *H*), 6.26 (d, J = 16.6 Hz, 1H, olefinic *H*), 6.18 (s, 2H, NH_2). ^{13}C NMR (101 MHz, DMSO-d_6) δ 148.94, 143.94, 128.19, 123.19, 119.72, 118.45, 93.52.

*1.9 (E)-3-(4-amino-3,5-difluorophenyl)acrylonitrile (**6b**).* Synthesized following general procedure 1.1. Yield 65%, white solid. ^{1}H NMR (400 MHz, DMSO-d_6) δ 7.42 (d, J = 16.5 Hz, 1H, olefinic *H*), 7.36 – 7.26 (m, 2H, Ar*H*), 6.21 (d, J = 16.5 Hz, 1H, olefinic *H*), 5.96 (s, 2H, NH_2). ^{13}C NMR (101 MHz, DMSO-d_6) δ 152.10 (d, $J_{C\text{-}F}$ = 10.0 Hz), 149.84 – 149.62 (m), 129.29 (t, $J_{C\text{-}F}$ = 16.9 Hz), 120.41 (t, $J_{C\text{-}F}$ = 8.9 Hz), 119.71, 111.35 (dd, $J_{C\text{-}F}$ = 14.5, 7.2 Hz), 93.33.

*1.10 (E)-3-(4-amino-3-fluoro-5-methylphenyl)acrylonitrile (**6c**).* Synthesized following general procedure 1.1. Yield 85%, pale yellow solid. ^{1}H NMR (400 MHz, DMSO-d_6) δ 7.38 (d, J = 16.5 Hz, 1H, olefinic *H*), 7.28 (d, $J_{H\text{-}F}$ = 12.3 Hz, 1H, Ar*H*), 7.11 (s, 1H, Ar*H*), 6.07 (d, J = 16.5 Hz, 1H, olefinic *H*), 5.63 (s, 2H, NH_2), 2.12 (s, 3H, CH_3). ^{13}C NMR (101 MHz, DMSO-d_6) δ 150.45 (d, $J_{C\text{-}F}$ = 237.7 Hz), 150.71 (d, $J_{C\text{-}F}$ = 2.6 Hz), 138.37 (d, $J_{C\text{-}F}$ =

12.6 Hz), 127.00, 123.82 (d, $J_{C\text{-}F}$ = 4.8 Hz), 121.47 (d, $J_{C\text{-}F}$ = 7.8 Hz), 120.22, 111.93 (d, $J_{C\text{-}F}$ = 19.1 Hz), 91.18, 17.65 (d, $J_{C\text{-}F}$ = 3.0 Hz).

*1.11 (E)-3-(4-amino-3-methyl-5-nitrophenyl)acrylonitrile (**6d**).* Synthesized following general procedure 1.1. Yield 59%, yellow solid. ^{1}H NMR (400 MHz, DMSO-d_6) δ 8.12 (s, 1H, Ar*H*), 7.70 (s, 1H, Ar*H*), 7.59 (s, 2H, NH_2), 7.51 (d, *J* = 16.6 Hz, 1H, olefinic *H*), 6.22 (d, *J* = 16.6 Hz, 1H, olefinic *H*), 2.22 (s, 3H, CH_3). ^{13}C NMR (101 MHz, DMSO-d_6) δ 149.57, 146.63, 133.18, 130.75, 127.74, 125.77, 121.37, 119.73, 93.69, 18.50.

*1.12 (E)-3-(4-amino-3,5-dimethylphenyl)acrylonitrile (**6e**).* Synthesized following general procedure 1.1. Yield 69%, pale yellow solid. ^{1}H NMR (400 MHz, DMSO-d_6) δ 7.31 (d, *J* = 16.4 Hz, 1H, olefinic *H*), 7.13 (s, 2H, Ar*H*), 5.92 (d, *J* = 16.5 Hz, 1H, olefinic *H*), 5.31 (s, 2H, NH_2), 2.08 (s, 6H, CH_3×2). ^{13}C NMR (101 MHz, DMSO-d_6) δ 151.63, 148.54, 128.61, 121.68, 120.90, 120.76, 88.81, 18.18.

*1.13 (E)-3-(4-amino-3-chloro-5-fluorophenyl)acrylonitrile (**6f**).* Synthesized following general procedure 1.1. Yield 78%, red-brown solid. ^{1}H NMR (400 MHz, DMSO-d_6) δ 7.49 – 7.38 (m, 3H, Ar*H* and olefinic *H*), 6.21 (d, *J* = 16.5 Hz, 1H, olefinic *H*), 6.11 (s, 2H, NH_2). ^{13}C NMR (101 MHz, DMSO-d_6) δ 151.74, 149.38 (d, $J_{C\text{-}F}$ = 2.6 Hz), 137.07 (d, $J_{C\text{-}F}$ = 16.0 Hz), 126.08 (d, $J_{C\text{-}F}$ = 1.7 Hz), 121.87 (d, $J_{C\text{-}F}$ = 8.2 Hz), 119.73, 118.26 (d, $J_{C\text{-}F}$ = 6.5 Hz), 112.92 (d, $J_{C\text{-}F}$ = 19.5 Hz), 93.34.

*1.14 6-fluoroquinazoline-2,4-diol (**9b**).* Synthesized following general procedure 1.2. Yield 86%, white solid. ^{1}H NMR (400 MHz, DMSO-d_6) δ 11.38 (s, 1H, O*H*), 11.17 (s, 1H, O*H*), 7.70 – 7.37 (m, 2H, Ar*H*), 7.22 – 7.14 (m, 1H, Ar*H*). ^{13}C NMR (101 MHz, $CDCl_3$) δ 162.56 (d, $J_{C\text{-}F}$ = 2.6 Hz), 157.75 (d, $J_{C\text{-}F}$ = 239.7 Hz), 150.51, 137.99, 123.33 (d, $J_{C\text{-}F}$ = 24.3 Hz), 118.02 (d, $J_{C\text{-}F}$ = 7.8 Hz), 115.84 (d, $J_{C\text{-}F}$ = 7.4 Hz), 112.40 (d, $J_{C\text{-}F}$ = 23.8 Hz).

*1.15 6-methoxyquinazoline-2,4-diol (**9d**).* Synthesized following general procedure 1.2. Yield 68%, off-white solid. ^{1}H NMR (400 MHz, DMSO-d_6) δ 11.24 (s, 1H, O*H*), 10.99 (s, 1H, O*H*), 7.32 (d, *J* = 2.7 Hz, 1H, Ar*H*), 7.29 – 7.24 (m, 1H, Ar*H*), 7.11 (d, *J* = 8.8 Hz, 1H, Ar*H*), 3.78 (s, 3H, CH_3). ^{13}C NMR (101 MHz, DMSO-d_6) δ 163.18, 155.07, 150.54, 135.43, 124.24, 117.39, 115.30, 108.51, 55.99.

*1.16 (E)-3-(4-((2-chloroquinazolin-4-yl)amino)-3,5-dimethylphenyl)acrylonitrile (**11u**).*

Synthesized following general procedure 1.3. Yield 23%, white solid. ^{1}H NMR (400 MHz, DMSO-d_6) δ 10.15 (s, 1H, N*H*), 8.54 (d, J = 8.1 Hz, 1H, Ar*H*), 7.89 (t, J = 7.6 Hz, 1H, Ar*H*), 7.72 (d, J = 8.2 Hz, 1H, Ar*H*), 7.68 –

7.58 (m, 2H, Ar*H* and olefinic *H*), 7.51 (s, 2H, Ar*H*), 6.47 (d, J = 16.8 Hz, 1H, olefinic *H*), 2.18 (s, 6H, CH_3×2). ^{13}C NMR (101 MHz, DMSO-d_6) δ 160.38, 156.74, 150.62, 150.12, 137.73, 136.50, 134.14, 132.56, 127.43, 126.80, 126.66, 123.42, 118.85, 113.17, 109.49, 96.74, 18.00. LCMS (ESI, M+1): 335.2.

*1.17 (E)-4-((6-chloro-4-((2,6-dichloro-4-(2-cyanovinyl)phenyl)amino)quinazolin-2-yl)amino) benzonitrile (**12a**)*. Synthesized following general procedure 1.4. Yield 41%, white solid, mp >325 °C (from *n*-butanol). ^{1}H NMR (400 MHz, DMSO-d_6) δ 11.61 (s, 1H, N*H*), 10.76 (s, 1H, N*H*), 8.84 (s, 1H, Ar*H*), 8.07 (s, 2H, Ar*H*), 7.96 (d, *J* = 8.6 Hz, 1H, Ar*H*), 7.82 – 7.69 (m, 2H, Ar*H* and olefinic *H*), 7.53 (s, 4H), 6.81 (d, *J* = 16.8 Hz, 1H, olefinic *H*). ^{13}C NMR (101 MHz, DMSO-d_6) δ 160.18, 153.38, 147.77, 142.99, 136.15, 135.04, 134.80, 133.15, 129.23, 128.31, 124.17, 120.72, 119.44, 118.63, 111.85, 105.25, 101.11. HRMS calcd for $C_{24}H_{13}Cl_3N_6$ $[M+H]^+$: 491.0340, found: 491.0338. HPLC analysis: retention time = 21.15 min; peak area, 96.42%.

*1.18 (E)-4-((6-chloro-4-((4-(2-cyanovinyl)-2,6-difluorophenyl)amino)quinazolin-2-yl)amino) benzonitrile(**12b**)*. Synthesized following general procedure 1.4. Yield 42%, yellow solid, mp 285-289 °C (from *n*-butanol). ^{1}H NMR (400 MHz, DMSO-d_6) δ 11.25 (s, 1H, N*H*), 10.68 (s, 1H, N*H*), 8.82 (s, 1H, Ar*H*), 7.98 – 7.90 (m, 1H, Ar*H*), 7.80 – 7.70 (m, 4H, Ar*H* and olefinic *H*), 7.62 (s, 4H, Ar*H*), 6.75 (d, *J* = 16.6 Hz, 1H, olefinic *H*). ^{13}C NMR (101 MHz, DMSO-d_6) δ 160.33, 159.60 (d, $J_{C\text{-}F}$ = 5.4 Hz), 157.12 (d, $J_{C\text{-}F}$ = 5.3 Hz), 153.62, 148.36, 143.07, 136.06, 135.46 (t, $J_{C\text{-}F}$ = 10.2 Hz), 133.25, 129.15, 124.25, 120.85, 119.50, 118.61, 116.86 (t, $J_{C\text{-}F}$ = 15.4 Hz), 112.06 (d, $J_{C\text{-}F}$ = 23.4 Hz), 105.24 (t, $J_{C\text{-}F}$ = 7.8 Hz), 100.64. HRMS calcd for $C_{24}H_{13}ClF_2N_6$ $[M+H]^+$: 459.0931, found: 459.0928. HPLC analysis: retention time = 20.49 min; peak area, 98.30%.

*1.19 (E)-4-((6-chloro-4-((4-(2-cyanovinyl)-2-fluoro-6-methylphenyl)amino)quinazolin-2-yl)amino)benzonitrile(**12c**)*. Synthesized following general procedure 1.4. Yield 52%, yellow solid, mp 278-282 °C (from *n*-butanol). ^{1}H NMR (400 MHz, DMSO-d_6) δ 10.98 (s, 1H, N*H*), 10.56 (s, 1H, N*H*), 8.81 – 8.74 (m, 1H, N*H*), 8.04 – 7.52 (m, 9H, Ar*H* and olefinic *H*), 6.36 (d, 14.2 Hz, 1H, olefinic *H*), 2.31 (s, 3H, CH_3). ^{13}C NMR (101 MHz, DMSO-d_6) δ 160.29, 157.06, 149.47 (d, $J_{C\text{-}F}$ = 2.5 Hz), 143.22, 139.19, 135.79, 134.84, 133.44 (d, $J_{C\text{-}F}$ = 11.7 Hz), 133.17, 129.01, 126.65 (d, $J_{C\text{-}F}$ = 2.1 Hz), 124.20, 120.54, 119.51, 118.96, 112.63 (d, $J_{C\text{-}F}$ = 22.0 Hz), 112.17, 99.10, 18.12 (d, $J_{C\text{-}F}$ = 2.3 Hz). HRMS calcd for $C_{25}H_{16}ClFN_6$ $[M+H]^+$: 455.1182, found: 455.1168. HPLC analysis: retention time = 19.25 min; peak area, 95.01%.

*1.20 (E)-4-((6-chloro-4-((4-(2-cyanovinyl)-2-methyl-6-nitrophenyl)amino)quinazolin-2-yl)amino)benzonitrile(**12d**).* Synthesized following general procedure 1.4. Yield 51%, yellow solid, mp 324-326 °C (from *n*-butanol). ^{1}H NMR (400 MHz, DMSO-d_6) δ11.56 (s, 1H, N*H*), 10.72 (s, 1H, N*H*), 8.84 (s, 1H, Ar*H*), 8.31 (s, 1H, Ar*H*), 8.14 (s, 1H, Ar*H*), 7.99 – 7.70 (m, 3H, Ar*H* and olefinic *H*), 7.62 – 7.42 (m, 4H, Ar*H*), 6.79 (d, *J* = 16.5 Hz, 1H, olefinic *H*), 2.37 (s, 3H, CH_3). ^{13}C NMR (101 MHz, DMSO-d_6) δ 160.29, 153.01, 148.34, 147.66, 142.75, 140.23, 136.22, 134.54, 134.32, 133.18, 131.50, 129.34, 124.37, 123.18, 122.50, 120.88, 119.41, 118.73, 112.11, 105.46, 100.66, 18.45. HRMS calcd for $C_{25}H_{16}ClN_7O_2$ $[M+H]^+$: 482.1127, found: 482.1125. HPLC analysis: retention time = 19.08 min; peak area, 95.05%.

*1.21 (E)-4-((4-((2,6-dichloro-4-(2-cyanovinyl)phenyl)amino)-6-fluoroquinazolin-2-yl)amino) benzonitrile (**12e**)*. Synthesized following general procedure 1.4. Yield 49%, pale yellow solid, mp >325 °C (from *n*-butanol). ^{1}H NMR (400 MHz, DMSO-d_6) δ 11.28 (s, 1H, N*H*), 10.53 (s, 1H, N*H*), 8.51 (d, *J* = 8.9 Hz, 1H, Ar*H*), 8.15 – 7.99 (m, 2H, Ar*H*), 7.97 – 7.48 (m, 7H, Ar*H* and olefinic *H*), 6.80 (d, *J* = 16.8 Hz, 1H, olefinic *H*). ^{13}C NMR (101 MHz, DMSO-d_6) δ 160.34 (d, $J_{C\text{-}F}$ = 3.2 Hz), 158.53 (d, $J_{C\text{-}F}$ = 244.2 Hz), 151.73, 147.22, 141.85, 135.87, 134.23, 133.13, 132.86, 132.70, 127.84, 125.06 (d, $J_{C\text{-}F}$ = 25.1 Hz), 122.34 (d, $J_{C\text{-}F}$ = 8.4 Hz), 120.64, 118.78, 118.11, 110.68 (d, $J_{C\text{-}F}$ = 8.9 Hz), 109.93 (d, $J_{C\text{-}F}$ = 24.3 Hz), 105.41, 100.77, 40.15, 39.94, 39.73, 39.52, 39.31, 39.10, 38.89. HRMS calcd for $C_{24}H_{13}Cl_2FN_6$ $[M+H]^+$: 475.0636, found: 475.0630. HPLC analysis: retention time = 17.83 min; peak area, 95.10%.

*1.22 (E)-4-((4-((2-chloro-4-(2-cyanovinyl)-6-fluorophenyl)amino)-6-fluoroquinazolin-2-yl)amino)benzonitrile(**12f**).* Synthesized following general procedure 1.4. Yield 45%, white solid, mp 297-299 °C (from *n*-butanol). ^{1}H NMR (400 MHz, DMSO-d_6) δ 11.53 (s, 1H, N*H*), 10.78 (s, 1H, N*H*), 8.64 (s, 1H, Ar*H*), 7.93 – 7.85 (m, 3H, Ar*H*), 7.82 – 7.72 (m, 2H, Ar*H* and olefinic *H*), 7.55 (dd, *J* = 20.5, 8.3 Hz, 4H, Ar*H*), 6.78 (d, *J* = 16.8 Hz, 1H, olefinic *H*). ^{13}C NMR (101 MHz, DMSO-d_6) δ 160.89 (d, $J_{C\text{-}F}$ = 3.1 Hz), 160.09 (d, $J_{C\text{-}F}$ = 5.5 Hz), 157.63 (d, $J_{C\text{-}F}$ = 11.7 Hz), 152.76, 148.05, 142.73, 136.19 (d, $J_{C\text{-}F}$ = 9.1 Hz), 133.99, 133.96, 133.22, 125.78, 125.75, 125.26 (d, $J_{C\text{-}F}$ = 23.9 Hz), 123.47, 121.02, 119.39, 118.59, 114.53 (d, $J_{C\text{-}F}$ = 21.7 Hz), 111.41 (d, $J_{C\text{-}F}$ = 8.7 Hz), 110.14 (d, $J_{C\text{-}F}$ = 26.6 Hz), 105.54, 100.96. HRMS calcd for $C_{24}H_{13}ClF_2N_6$ $[M+H]^+$: 459.0931, found: 459.0932. HPLC analysis: retention time = 17.58 min; peak area, 98.35%.

*1.23 (E)-4-((4-((4-(2-cyanovinyl)-2,6-difluorophenyl)amino)-6-fluoroquinazolin-2-yl)amino) benzonitrile(**12g**).* Synthesized following general procedure 1.4. Yield 48%, pale yellow solid, mp 293-299 °C (from *n*-butanol). ^{1}H NMR (400 MHz, DMSO-d_6) δ 10.98 (s, 1H, N*H*), 10.52 (s, 1H, N*H*), 8.51 (d, J = 9.0 Hz, 1H, Ar*H*), 8.14 – 7.69 (m, 6H, Ar*H* and olefinic *H*), 7.69 – 7.58 (m, 3H, Ar*H*), 6.74 (d, J = 16.6 Hz, 1H, olefinic *H*). ^{13}C NMR (101 MHz, DMSO-d_6) δ 160.64, 159.88, 159.69, 157.46, 157.19 (d, $J_{C\text{-}F}$ = 4.8 Hz), 153.66, 148.38, 143.50, 133.47 (d, $J_{C\text{-}F}$ = 16.5 Hz), 133.22, 124.94, 124.68, 123.84, 120.51, 119.61, 118.62, 112.05 (d, $J_{C\text{-}F}$ = 24.3 Hz), 111.72, 109.61 (d, $J_{C\text{-}F}$ = 24.5 Hz), 106.58, 104.77, 104.68, 100.56. HRMS calcd for $C_{24}H_{13}F_3N_6$ $[M+H]^+$: 443.1227, found: 443.1218. HPLC analysis: retention time = 16.99 min; peak area, 95.05%.

*1.24 (E)-4-((4-((4-(2-cyanovinyl)-2-fluoro-6-methylphenyl)amino)-6-fluoroquinazolin-2-yl)amino)benzonitrile(**12h**).* Synthesized following general procedure 1.4. Yield 47%, pale yellow solid, mp 284-288 °C (from *n*-butanol). ^{1}H NMR (400 MHz, DMSO-d_6) δ 11.60 (s, 1H, N*H*), 10.91 (s, 1H, N*H*), 8.78 (d, J = 9.0 Hz, 1H, Ar*H*), 8.12 – 7.67 (m, 5H, Ar*H* and olefinic *H*), 7.59 – 7.51 (m, 3H, Ar*H*), 7.50 – 7.44 (m, 2H, Ar*H*), 6.67 (d, J = 16.6 Hz, 1H, olefinic *H*), 2.32 (s, 3H, CH_3). ^{13}C NMR (101 MHz, DMSO-d_6) δ 160.99 (d, $J_{C\text{-}F}$ = 3.2 Hz), 160.23, 158.171 (d, $J_{C\text{-}F}$ = 248.9 Hz), 157.80, 152.07, 149.39, 142.29, 139.14, 135.17 (d, $J_{C\text{-}F}$ = 8.7 Hz), 133.22, 126.66, 126.31 (d, $J_{C\text{-}F}$ = 13.4 Hz), 125.22 (d, $J_{C\text{-}F}$ = 24.3 Hz), 122.16 (d, $J_{C\text{-}F}$ = 6.2 Hz), 121.11, 119.10 (d, $J_{C\text{-}F}$ = 36.8 Hz), 112.63 (d, $J_{C\text{-}F}$ = 21.7 Hz), 111.58 (d, $J_{C\text{-}F}$ = 8.7 Hz), 110.73 (d, $J_{C\text{-}F}$ = 25.1 Hz), 105.92, 99.27, 18.11 (d, $J_{C\text{-}F}$ = 2.2 Hz). HRMS calcd for $C_{25}H_{16}F_2N_6$ $[M+H]^+$: 439.1477, found: 439.1470. HPLC analysis: retention time = 15.42 min; peak area, 95.05%.

*1.25 (E)-4-((4-((4-(2-cyanovinyl)-2-methyl-6-nitrophenyl)amino)-6-fluoroquinazolin-2-yl)amino)benzonitrile(**12i**).* Synthesized following general procedure 1.4. Yield 47%, yellow solid, mp 294-298 °C (from *n*-butanol). ^{1}H NMR (400 MHz, DMSO-d_6) δ 11.73 (s, 1H, N*H*), 10.78 (s, 1H, N*H*), 8.66 (d, J = 8.8 Hz, 1H, Ar*H*), 8.31 (s, 1H, Ar*H*), 8.14 (s, 1H, Ar*H*), 7.90 – 7.44 (m, 7H, Ar*H* and olefinic *H*), 6.80 (d, J = 16.6 Hz, 1H, olefinic *H*), 2.38 (s, 3H, CH_3). ^{13}C NMR (101 MHz, DMSO-d_6) δ 160.80, 158.92 (d, $J_{C\text{-}F}$ = 242.1 Hz), 152.42, 148.31, 147.69, 142.57, 140.22, 134.56, 134.42, 133.60, 133.37, 133.19, 131.35, 122.50, 121.01, 119.36, 118.72, 111.57, 105.64, 100.72, 18.44. HRMS calcd for $C_{25}H_{16}FN_7O_2$ $[M+H]^+$: 466.1416, found: 466.1421. HPLC analysis: retention time = 15.48 min; peak area, 95.01%.

*1.26 (E)-4-((4-((4-(2-cyanovinyl)-2,6-dimethylphenyl)amino)-6-methoxyquinazolin-2-yl)amino) benzonitrile **(12j)***. Synthesized following general procedure 1.4. Yield 46%, pale yellow solid, mp 303-308 °C (from *n*-butanol). ^{1}H NMR (400 MHz, DMSO-d_6) δ 11.45 (s, 1H, N*H*), 10.77 (s, 1H, N*H*), 8.32 (s, 1H, Ar*H*), 7.75 (d, *J* = 16.8 Hz, 1H, olefinic *H*), 7.69 – 7.54 (m, 4H, Ar*H*), 7.42 (dd, *J* = 22.6, 8.5 Hz, 4H, Ar*H*), 6.58 (d, *J* = 16.8 Hz, 1H, olefinic *H*), 3.96 (s, 3H, OCH_3), 2.23 (s, 6H, CH_3×2). ^{13}C NMR (101 MHz, $CDCl_3$) δ 160.58, 157.22, 150.98, 150.57, 142.68, 138.11, 136.84, 133.71, 133.17, 128.94, 128.06, 126.40, 120.81, 120.28, 119.32, 111.33, 106.11, 105.35, 97.64, 56.86, 18.41. HRMS calcd for $C_{27}H_{22}N_6O$ $[M+H]^+$: 447.1928, found: 447.1940. HPLC analysis: retention time = 12.95 min; peak area, 97.30%.

*1.27 (E)-4-((4-((2,6-dichloro-4-(2-cyanovinyl)phenyl)amino)-6-methoxyquinazolin-2-yl)amino) benzonitrile(**12k**)*. Synthesized following general procedure 1.4. Yield 47%, yellow solid, mp 156-159 °C (from *n*-butanol). ^{1}H NMR (400 MHz, DMSO-d_6) δ 11.95 (s, 1H, N*H*), 10.90 (s, 1H, N*H*), 8.33 (s, 1H, Ar*H*), 8.15 (s, 2H, Ar*H*), 7.69 (dd, *J* = 31.4, 8.5 Hz, 2H, Ar*H*), 7.59 (d, *J* = 12.1 Hz, 1H, olefinic *H*), 7.49 (dd, *J* = 38.1, 8.4 Hz, 4H, Ar*H*), 6.26 (d, *J* = 12.1 Hz, 1H, olefinic *H*), 3.96 (s, 3H, OCH_3). ^{13}C NMR (101 MHz, DMSO-d_6) δ 160.86, 157.37, 150.98, 145.96, 142.39, 136.35, 136.12, 134.80, 134.65, 133.44, 133.17, 129.09, 127.27, 121.28, 120.74, 119.21, 117.53, 111.02, 105.72, 100.23, 56.90. HRMS calcd for $C_{25}H_{16}Cl_2N_6O$ $[M+H]^+$: 487.0835, found: 487.0837. HPLC analysis: retention time = 17.97 min; peak area, 95.03%.

*1.28 (E)-4-((4-((4-(2-cyanovinyl)-2,6-difluorophenyl)amino)-6-methoxyquinazolin-2-yl)amino) benzonitrile(**12l**)*. Synthesized following general procedure 1.4. Yield 53%, pale yellow solid, mp 301-305 °C (from *n*-butanol). ^{1}H NMR (400 MHz, DMSO-d_6) δ 11.67 (s, 1H, N*H*), 10.85 (s, 1H, N*H*), 8.31 (s, 1H, Ar*H*), 7.79 – 7.67 (m, 4H, Ar*H* and olefinic *H*), 7.66 – 7.47 (m, 5H, Ar*H*), 6.76 (d, *J* = 16.6 Hz, 1H, olefinic *H*), 3.94 (s, 3H, OCH_3). ^{13}C NMR (101 MHz, DMSO-d_6) δ 161.02, 159.58 (d, $J_{C\text{-}F}$ = 5.0 Hz), 157.29, 157.10 (d, $J_{C\text{-}F}$ = 5.5 Hz), 151.15, 148.29, 142.33, 135.74 (t, $J_{C\text{-}F}$ = 9.0 Hz), 133.28, 127.27, 121.17, 119.33, 118.58, 116.63 (t, $J_{C\text{-}F}$ = 17.7 Hz), 112.08 (d, $J_{C\text{-}F}$ = 23.8 Hz), 111.38, 105.88, 105.71, 100.78, 56.90. HRMS calcd for $C_{25}H_{16}F_2N_6O$ $[M+H]^+$: 455.1426, found: 455.1417. HPLC analysis: retention time = 13.89 min; peak area, 96.94%.

*1.29 (E)-4-((4-((4-(2-cyanovinyl)-2,6-difluorophenyl)amino)-6-hydroxyquinazolin-2-yl)amino) benzonitrile(**12m**)*. Compound **12m** was synthesized via a known demethylation procedure[47, 61] of **12l**, not from

intermediate **11m**. Yield 41%, yellow solid, mp >325 °C (from *n*-butanol). ^{1}H NMR (400 MHz, DMSO-d_6) δ 9.79 (s, 1H, N*H*), 9.69 (s, 1H, N*H*), 9.54 (s, 1H, O*H*), 7.87 – 7.59 (m, 6H, Ar*H* and olefinic *H*), 7.59 – 7.45 (m, 3H, Ar*H*), 7.41 – 7.32 (m, 1H, Ar*H*), 6.70 (d, J = 16.5 Hz, 1H, olefinic *H*). ^{13}C NMR (101 MHz, DMSO-d_6) δ 160.07, 159.63, 157.59, 154.18, 153.87, 148.61, 145.62, 134.42, 133.11, 126.66, 125.78, 120.15, 118.73, 112.47, 111.94 (d, $J_{C\text{-}F}$ = 23.4 Hz), 110.01, 106.44, 102.29, 100.06. HRMS calcd for $C_{24}H_{14}F_2N_6O$ $[M+H]^+$: 441.1270, found: 441.1265. HPLC analysis: retention time = 10.23 min; peak area, 95.04%.

*1.30 (E)-4-((4-((4-(2-cyanovinyl)-2,6-difluorophenyl)amino)-6-nitroquinazolin-2-yl)amino) benzonitrile(**12n**).* Synthesized following general procedure 1.4. Yield 47%, yellow solid, mp 320-325 °C (from *n*-butanol). ^{1}H NMR (400 MHz, DMSO-d_6) δ 10.96 (s, 1H, N*H*), 10.42 (s, 1H, N*H*), 9.55 (s, 1H, Ar*H*), 8.51 (d, J = 8.9 Hz, 1H, Ar*H*), 7.84 – 7.66 (m, 6H, Ar*H* and olefinic *H*), 7.65 – 7.55 (m, 2H, Ar*H*), 6.74 (d, J = 16.6 Hz, 1H, olefinic *H*). ^{13}C NMR (101 MHz, DMSO-d_6) δ 161.27, 159.69 (d, $J_{C\text{-}F}$ = 5.2 Hz), 157.21 (d, $J_{C\text{-}F}$ = 5.5 Hz), 148.44, 144.11, 142.69, 135.08 (t, $J_{C\text{-}F}$ = 9.6 Hz), 133.92, 133.17, 128.58, 125.88, 122.02, 120.18, 119.70, 118.66, 117.31 (t, $J_{C\text{-}F}$ = 16.2 Hz), 112.07 (d, $J_{C\text{-}F}$ = 23.8 Hz), 110.71, 104.35, 100.44. HRMS calcd for $C_{24}H_{13}F_2N_7O_2$ $[M+Na]^+$: 492.0991, found: 492.0995. HPLC analysis: retention time = 20.72 min; peak area, 98.63%.

*1.31 (E)-4-((7-chloro-4-((2,6-dichloro-4-(2-cyanovinyl)phenyl)amino)quinazolin-2-yl)amino) benzonitrile(**12o**)*. Synthesized following general procedure 1.4. Yield 55%, pale yellow solid, mp >325 °C (from *n*-butanol). ^{1}H NMR (400 MHz, DMSO-d_6) δ 11.02 (s, 1H, N*H*), 10.37 (s, 1H, N*H*), 8.54 (d, J = 8.7 Hz, 1H, Ar*H*), 8.05 (s, 2H, Ar*H*), 7.81 – 7.47 (m, 7H, Ar*H* and olefinic *H*), 6.79 (d, J = 16.6 Hz, 1H, olefinic *H*). ^{13}C NMR (101 MHz, DMSO-d_6) δ 160.70, 153.40, 147.74, 142.76, 140.82, 136.20, 135.03, 134.82, 133.13, 128.29, 127.05, 125.78, 120.97, 120.40, 119.37, 118.61, 109.54, 105.51, 101.15. HRMS calcd for $C_{24}H_{13}Cl_3N_6$ $[M+H]^+$: 491.0340, found: 491.0333. HPLC analysis: retention time = 15.42 min; peak area, 95.03%.

*1.32 (E)-4-((7-chloro-4-((2-chloro-4-(2-cyanovinyl)-6-fluorophenyl)amino)quinazolin-2-yl)amino)benzonitrile(**12p**).* Synthesized following general procedure 1.4. Yield 40%, white solid, mp 304-306 °C (from *n*-butanol). ^{1}H NMR (400 MHz, DMSO-d_6) δ 11.24 (s, 1H, N*H*), 10.69 (s, 1H, N*H*), 8.67 (d, J = 8.8 Hz, 1H, Ar*H*), 7.91 (s, 1H, Ar*H*), 7.87 (d, J = 10.4 Hz, 1H, Ar*H*), 7.79 – 7.71 (m, 2H, Ar*H* and olefinic *H*), 7.68 – 7.50 (m, 5H, Ar*H*), 6.77 (d, J = 16.8 Hz, 1H, olefinic *H*). ^{13}C NMR (101 MHz, DMSO-d_6) δ 160.81, 160.16,

157.65, 153.89, 148.08, 140.58, 136.05 (d, J_{C-F} = 9.1 Hz), 134.08 (d, J_{C-F} = 2.9 Hz), 133.17, 126.97, 125.65 (d, J_{C-F} = 21.6 Hz), 120.88, 119.46, 118.61, 114.50 (d, J_{C-F} = 21.8 Hz), 109.82, 100.88. HRMS calcd for $C_{24}H_{13}Cl_2FN_6$ $[M+H]^+$: 475.0636, found: 475.0632. HPLC analysis: retention time = 20.95 min; peak area, 95.10%.

*1.33 (E)-4-((7-chloro-4-((4-(2-cyanovinyl)-2,6-difluorophenyl)amino)quinazolin-2-yl)amino) benzonitrile(**12q**).* Synthesized following general procedure 1.4. Yield 49%, white solid, mp 318-322 °C (from *n*-butanol). ^{1}H NMR (400 MHz, DMSO-d_6) δ 10.59 (s, 1H, N*H*), 10.21 (s, 1H, N*H*), 8.50 (d, *J* = 8.7 Hz, 1H, Ar*H*), 7.81 – 7.68 (m, 4H, Ar*H* and olefinic *H*), 7.66 – 7.54 (m, 5H, Ar*H*), 6.73 (d, *J* = 16.6 Hz, 1H, olefinic *H*). ^{13}C NMR (101 MHz, DMSO-d_6) δ 160.79, 159.68 (d, J_{C-F} = 5.7 Hz), 157.20 (d, J_{C-F} = 5.5 Hz), 154.23, 148.36, 143.23, 140.41, 135.40 (t, J_{C-F} = 9.0 Hz), 133.44 (d, J_{C-F} = 19.0 Hz), 133.21, 126.93, 125.37, 120.83, 119.53, 118.61, 116.99 (t, J_{C-F} = 16.7 Hz), 112.04 (d, J_{C-F} = 23.8 Hz), 110.07, 105.11, 100.60. HRMS calcd for $C_{24}H_{13}ClF_2N_6$ $[M+H]^+$: 459.0931, found: 459.0932. HPLC analysis: retention time = 25.58 min; peak area, 98.28%.

*1.34 (E)-4-((7-chloro-4-((4-(2-cyanovinyl)-2-fluoro-6-methylphenyl)amino)quinazolin-2-yl)amino)benzonitrile(**12r**).* Synthesized following general procedure 1.4. Yield 43%, white solid, mp 248-251 °C (from *n*-butanol). ^{1}H NMR (400 MHz, DMSO-d_6) δ 11.37 (s, 1H, N*H*), 10.82 (s, 1H, N*H*), 8.77 (d, *J* = 8.8 Hz, 1H, Ar*H*), 7.79 – 7.61 (m, 4H, Ar*H* and olefinic *H*), 7.58 – 7.50 (m, 5H, Ar*H*), 6.66 (d, *J* = 16.6 Hz, 1H, olefinic *H*), 2.30 (s, 3H, CH_3). ^{13}C NMR (101 MHz, DMSO-d_6) δ 160.89, 158.25 (d, J_{C-F} = 247.5 Hz), 153.20, 149.45, 142.69, 140.63, 139.21, 135.03 (d, J_{C-F} = 8.7 Hz), 133.18, 127.29, 126.65, 126.52, 125.66, 120.99, 119.75, 119.16 (d, J_{C-F} = 43.8 Hz), 112.63 (d, J_{C-F} = 21.7 Hz), 109.89, 105.59, 99.19, 18.11 (d, J_{C-F} = 2.0 Hz). HRMS calcd for $C_{25}H_{16}ClFN_6$ $[M+H]^+$: 455.1182, found: 455.1182. HPLC analysis: retention time = 23.80 min; peak area, 95.19%.

*1.35 (E)-4-((7-chloro-4-((4-(2-cyanovinyl)-2-methyl-6-nitrophenyl)amino)quinazolin-2-yl)amino)benzonitrile(**12s**).* Synthesized following general procedure 1.4. Yield 49%, yellow solid, mp 287-289 °C (from *n*-butanol). ^{1}H NMR (400 MHz, DMSO-d_6) δ 11.38 (s, 1H, N*H*), 10.62 (s, 1H, N*H*), 8.64 (d, *J* = 8.7 Hz, 1H, Ar*H*), 8.29 (s, 1H, Ar*H*), 8.12 (s, 1H, Ar*H*), 7.83 (d, *J* = 16.6 Hz, 1H, olefinic *H*), 7.75 (s, 1H, Ar*H*), 7.62 (d, *J* = 8.8 Hz, 1H, Ar*H*), 7.53 (s, 4H, Ar*H*), 6.77 (d, *J* = 16.6 Hz, 1H, olefinic *H*), 2.35 (s, 3H, CH_3). ^{13}C NMR (101 MHz, DMSO-d_6) δ 160.66, 153.76, 148.37, 147.73, 140.51, 140.23, 134.48, 134.20, 133.15, 127.01, 125.50,

122.48, 120.79, 119.48, 118.75, 110.04, 105.22, 100.59, 18.46. HRMS calcd for $C_{25}H_{16}ClN_7O_2$ $[M+H]^+$: 482.1127, found: 482.1122. HPLC analysis: retention time = 12.57 min; peak area, 95.01%.

*1.36 (E)-4-((4-((2-amino-4-(2-cyanovinyl)-6-methylphenyl)amino)-7-chloroquinazolin-2-yl)amino)benzonitrile(**12t**).* Compound **12t** was synthesized from reduction of **12s**, not from intermediate **11t**. Compound **12s** (482 mg, 1 mmol, 1.0 eq), zinc powder (327 mg, 5 mmol, 5.0 eq), NH_4Cl (535 mg, 10 mmol, 10.0eq) and ethanol/water (10 mL, v/v=1:1) was heated at 60 °C for 2 h, then the resulting mixture was filtered. The filtrate was diluted with ethyl acetate, and was washed with water. The organic layer was dried with anhydrous Na_2SO_4, concentrated. The residue was purified by a silica gel chromatography column. Yield 46%, yellow solid, mp 210-213 °C (from *n*-butanol). ^{1}H NMR (400 MHz, DMSO-d_6) δ 9.72 (s, 1H, N*H*), 9.47 (s, 1H, N*H*), 8.40 (d, *J* = 8.6 Hz, 1H, Ar*H*), 7.84 (d, *J* = 7.3 Hz, 2H, Ar*H*), 7.60 (d, *J* = 16.6 Hz, 1H, olefinic *H*), 7.53 (s, 1H, Ar*H*), 7.42 (d, *J* = 7.9 Hz, 2H, Ar*H*), 7.36 (d, *J* = 8.1 Hz, 1H, Ar*H*), 6.90 (s, 2H, Ar*H*), 6.32 (d, *J* = 16.6 Hz, 1H, olefinic *H*), 5.21 (s, 2H, NH_2), 2.09 (s, 3H, CH_3). ^{13}C NMR (101 MHz, DMSO-d_6) δ 160.62, 157.76, 152.93, 151.72, 146.64, 146.05, 138.17, 137.64, 133.27, 132.89, 126.42, 125.22, 124.56, 122.92, 120.19, 119.57, 118.84, 117.18, 112.56, 111.20, 101.98, 96.12, 18.60. HRMS calcd for $C_{25}H_{18}ClN_7$ $[M+H]^+$: 452.1385, found: 452.1381. HPLC analysis: retention time = 20.82 min; peak area, 95.41%.

*1.37 (E)-4-((4-((4-(2-cyanovinyl)-2,6-dimethylphenyl)amino)quinazolin-2-yl)amino) benzonitrile (**12u**).* Synthesized following general procedure 1.4. Yield 38%, white solid, mp 280-284 °C (from *n*-butanol). ^{1}H NMR (400 MHz, DMSO-d_6) δ 11.33 (s, 1H, N*H*), 10.85 (s, 1H, N*H*), 8.67 (d, *J* = 7.9 Hz, 1H, Ar*H*), 7.95 (t, *J* = 7.5 Hz, 1H, Ar*H*), 7.77 – 7.65 (m, 2H, Ar*H* and olefinic *H*), 7.64 – 7.55 (m, 3H, Ar*H*), 7.42 (dd, *J* = 19.3, 8.1 Hz, 4H, Ar*H*), 6.57 (d, *J* = 16.6 Hz, 1H, olefinic *H*), 2.21 (s, 6H, CH_3×2). ^{13}C NMR (101 MHz, DMSO-d_6) δ 160.49, 151.53, 150.05, 142.03, 137.54, 136.33, 135.88, 133.24, 132.66, 127.54, 125.26, 124.62, 120.01, 118.79, 110.23, 105.07, 97.17, 17.86. HRMS calcd for $C_{26}H_{20}N_6$ $[M+H]^+$: 417.1822, found: 417.1813. HPLC analysis: retention time = 15.03 min; peak area, 95.69%.

*1.38 (E)-4-((4-((2,6-dichloro-4-(2-cyanovinyl)phenyl)amino)quinazolin-2-yl)amino) benzonitrile(**12v**).* Synthesized following general procedure 1.4. Yield 52%, white solid, mp >325 °C (from *n*-butanol). ^{1}H NMR (400 MHz, DMSO-d_6) δ 11.73 (s, 1H, N*H*), 10.92 (s, 1H, N*H*), 8.67 (d, *J* = 8.2 Hz, 1H, Ar*H*), 8.09 (s, 2H, Ar*H*),

7.99 (t, *J* = 7.7 Hz, 1H, Ar*H*), 7.81 – 7.71 (m, 2H, Ar*H* and olefinic *H*), 7.63 (t, *J* = 7.6 Hz, 1H, Ar*H*), 7.51 (dd, *J* = 33.7, 8.4 Hz, 4H, Ar*H*), 6.83 (d, *J* = 16.6 Hz, 1H, olefinic *H*). ^{13}C NMR (101 MHz, DMSO-d_6) δ 161.23, 147.73, 142.38, 136.78, 136.33, 134.93, 134.78, 133.21, 128.32, 125.97, 125.07, 121.07, 119.29, 118.61, 110.46, 101.22. HRMS calcd for $C_{24}H_{14}Cl_2N_6$ $[M+H]^+$: 457.0730, found: 457.0729. HPLC analysis: retention time = 12.57 min; peak area, 99.09%.

*1.39 (E)-4-((4-((2-chloro-4-(2-cyanovinyl)-6-fluorophenyl)amino)quinazolin-2-yl)amino) benzonitrile(**12w**).* Synthesized following general procedure 1.4. Yield 51%, white solid, mp 304-308 °C (from *n*-butanol). ^{1}H NMR (400 MHz, DMSO-d_6) δ 11.63 (s, 1H, N*H*), 10.94 (s, 1H, N*H*), 8.69 (d, *J* = 8.2 Hz, 1H, N*H*), 7.97 (t, *J* = 7.8 Hz, 1H, Ar*H*)), 7.93 (s, 1H, Ar*H*)), 7.89 (d, *J* = 10.3 Hz, 1H, Ar*H*)), 7.78 – 7.72 (m, 2H, Ar*H* and olefinic *H*), 7.63 – 7.45 (m, 5H, Ar*H*)), 6.79 (d, *J* = 16.6 Hz, 1H, olefinic *H*). ^{13}C NMR (101 MHz, DMSO-d_6) δ 161.45, 160.06, 157.57, 152.34, 148.04, 142.30, 136.80, 136.26, 134.03 (d, $J_{C\text{-}F}$ = 2.7 Hz), 133.25, 125.86 (d, $J_{C\text{-}F}$ = 22.3 Hz), 125.18, 121.27, 118.94 (d, $J_{C\text{-}F}$ = 70.9 Hz), 114.54 (d, $J_{C\text{-}F}$ = 21.7 Hz), 110.62, 101.04. HRMS calcd for $C_{24}H_{14}ClFN_6$ $[M+H]^+$: 441.1025, found: 441.1018. HPLC analysis: retention time = 12.20 min; peak area, 97.85%.

*1.40 (E)-4-((4-((4-(2-cyanovinyl)-2,6-difluorophenyl)amino)quinazolin-2-yl)amino) benzonitrile(**12x**).* Synthesized following general procedure 1.4. Yield 39%, white solid, mp 306-312 °C (from *n*-butanol). ^{1}H NMR (400 MHz, DMSO-d_6) δ 11.74 (s, 1H, N*H*), 11.06 (s, 1H, N*H*), 8.76 (d, *J* = 7.9 Hz, 1H, Ar*H*), 7.98 (t, *J* = 1.8 Hz, 1H, Ar*H*), 7.84 – 7.71 (m, 4H, Ar*H* and olefinic *H*), 7.70 – 7.57 (m, 3H, Ar*H*), 7.55 – 7.47 (m, 2H, Ar*H*), 6.78 (d, *J* = 16.6 Hz, 1H, olefinic *H*). ^{13}C NMR (101 MHz, DMSO-d_6) δ 161.60, 159.59 (d, $J_{C\text{-}F}$ = 5.2 Hz), 157.10 (d, $J_{C\text{-}F}$ = 5.2 Hz), 152.11, 148.27, 142.02, 136.89, 135.87 (t, $J_{C\text{-}F}$ = 9.9 Hz), 133.31, 126.03, 125.42, 121.49, 119.43, 119.26, 118.57, 116.53 (t, $J_{C\text{-}F}$ = 17.0 Hz), 112.07 (d, $J_{C\text{-}F}$ = 23.4 Hz), 110.74, 106.30, 100.86. HRMS calcd for $C_{24}H_{14}F_2N_6$ $[M+H]^+$: 425.1321, found: 425.1314. HPLC analysis: retention time = 15.80 min; peak area, 95.49%.

*1.41 (E)-4-((4-((4-(2-cyanovinyl)-2-fluoro-6-methylphenyl)amino)quinazolin-2-yl)amino) benzonitrile(**12y**).* Synthesized following general procedure 1.4. Yield 50%, white solid, mp 286-292 °C (from *n*-butanol). ^{1}H NMR (400 MHz, DMSO-d_6) δ 11.33 (s, 1H, N*H*), 10.83 (s, 1H, N*H*), 8.69 (d, *J* = 7.9 Hz, 1H, Ar*H*), 8.08 – 7.47 (m, 10H, Ar*H* and olefinic *H*), 6.66 (d, *J* = 16.8 Hz, 1H, olefinic *H*), 2.31 (s, 3H, C*H*$_3$). ^{13}C NMR (101 MHz, DMSO-d_6) δ 161.38, 152.30, 149.43, 142.50, 139.24, 139.09, 136.49, 135.12 (d, $J_{C\text{-}F}$ = 9.7 Hz), 133.48 (d, $J_{C\text{-}F}$ = 17.8 Hz),

133.22, 126.64, 125.79, 125.08, 121.07, 119.15 (d, $J_{C\text{-}F}$ = 40.9 Hz), 112.63 (d, $J_{C\text{-}F}$ = 17.7 Hz), 110.79, 99.24, 18.04 (d, $J_{C\text{-}F}$ = 1.7 Hz). HRMS calcd for $C_{25}H_{17}FN_6$ $[M+H]^+$: 421.1571, found: 421.1568. HPLC analysis: retention time = 14.87 min; peak area, 95.04%.

*1.42 (E)-4-((4-((4-(2-cyanovinyl)-2-methyl-6-nitrophenyl)amino)quinazolin-2-yl)amino) benzonitrile(**12z**).* Synthesized following general procedure 1.4. Yield 53%, yellow solid, mp 285-288 °C (from *n*-butanol). ^{1}H NMR (400 MHz, DMSO-d_6) δ 11.51 (s, 1H, N*H*), 10.88 (s, 1H, N*H*), 8.67 (d, *J* = 7.9 Hz, 1H, Ar*H*), 8.31 (s, 1H, Ar*H*), 8.14 (s, 1H, Ar*H*), 8.02 – 7.91 (m, 1H, Ar*H*), 7.84 (d, *J* = 16.6 Hz, 1H, olefinic *H*), 7.71 (d, *J* = 8.2 Hz, 1H, Ar*H*), 7.62 (t, *J* = 7.3 Hz, 1H, Ar*H*), 7.57 – 7.32(m, 4H, Ar*H*), 6.79 (d, *J* = 16.8 Hz, 1H, olefinic *H*), 2.36 (s, 3H, CH_3). ^{13}C NMR (101 MHz, DMSO-d_6) δ 161.35, 152.15, 148.32, 147.76, 140.27, 136.71, 134.56, 133.21, 131.50, 125.95, 125.25, 122.49, 121.16, 119.30, 118.72, 110.81, 110.01, 105.97, 100.76, 18.40. HRMS calcd for $C_{25}H_{17}N_7O_2$ $[M+H]^+$: 448.1516, found: 448.1506. HPLC analysis: retention time = 10.55 min; peak area, 98.89%.

2. In Vitro Anti-HIV Assay.

Evaluation of the antiviral activity of the compounds against HIV in MT-4 cells was performed using the MTT assay as previously described.[62, 63] All used NNRTI-resistant strains were a gift of Prof. Jan Balzarini from Rega Institute for Medical Research, KU Leuven. All used strains were analyzed and reported earlier.[64 65, 66] Prior to use in our assays, every freshly grown virus stock is the subject of a genotypic analysis. Besides the genotypic analysis every stock is subject to a phenotypic analysis using a panel of relevant reference compounds in MT-4 cells. In the case of NNRTI-resistant strains the reference compounds used are NVP, EFV and ETR. Stock solutions (10 x final concentration) of test compounds were added in 25 µl volumes to two series of triplicate wells so as to allow simultaneous evaluation of their effects on mock- and HIV-infected cells at the beginning of each experiment. Serial 5-fold dilutions of test compounds were made directly in flat-bottomed 96-well microtiter trays using a Biomek 3000 robot (Beckman instruments, Fullerton, CA). Untreated HIV- and mock-infected cell samples were included as controls. HIV stock (50 µl) at 100-300 $CCID_{50}$ (50 % cell culture infectious doses) and culture medium (final 200 µL volume per well) were added to either the infected or mock-infected wells of the microtiter tray. Mock-infected cells were used to evaluate the effects of test compound on uninfected cells in

order to assess the cytotoxicity of the test compounds. Exponentially growing MT-4 cells were centrifuged for 5 minutes at 220 g and the supernatant was discarded. The MT-4 cells were resuspended at 6 x 10^5 cells/ml and 50 µl volumes were transferred to the microtiter tray wells. Five days after infection, the viability of mock-and HIV-infected cells was examined spectrophotometrically using the MTT assay. The MTT assay is based on the reduction of yellow colored 3-(4,5-dimethylthiazol-2-yl)-2,5-diphenyltetrazolium bromide (MTT) (Acros Organics) by mitochondrial dehydrogenase activity in metabolically active cells to a blue-purple formazan that can be measured spectrophotometrically. The absorbances were read in an eight-channel computer-controlled photometer (Infinite M1000, Tecan), at two wavelengths (540 and 690 nm). All data were calculated using the median absorbance value of three wells. The 50% cytotoxic concentration (CC_{50}) was defined as the concentration of the test compound that reduced the absorbance (OD540) of the mock-infected control sample by 50%. The concentration achieving 50% protection against the cytopathic effect of the virus in infected cells was defined as the 50% effective concentration (EC_{50}).

3. Reverse transcriptase assay.

Recombinant wild type p66/p51 HIV-1 RT was expressed and purified as described.[67] The RT assay was performed with the EnzCheck Reverse Transcriptase Assay kit (Molecular Probes, Invitrogen), as described by the Manufacturer. The assay is based on the dsDNA quantitation reagent PicoGreen. This reagent shows a pronounced increase in fluorescence signal upon binding to dsDNA or RNA-DNA heteroduplexes. Single-stranded nucleic acids generate only minor fluorescence signal enhancement when a sufficiently high dye:base pair ratio is applied.[68] This condition is met in the assay. A poly(rA) template of approximately 350 bases long, and an oligo(dT)16 primer, are annealed in a molar ratio of 1:1.2 (60 min at room temperature). Fifty-two ng of the RNA/DNA is brought into each well of a 96-well plate in a volume of 20 µl polymerization buffer (60 mM Tris-HCl, 60 mM KCl, 8 mM $MgCl_2$, 13 mM DTT, 100 µM dTTP, pH 8.1). Five µl of RT enzyme solution, diluted to a suitable concentration in enzyme dilution buffer (50 mM Tris-HCl, 20% glycerol, 2 mM DTT, pH

7.6), is added. The reactions are incubated at 25°C for 40 minutes and then stopped by the addition of EDTA (15 mM fc). Heteroduplexes are then detected by addition of PicoGreen. Signals are read using an excitation wavelength of 490 nm and emission detection at 523 nm using a spectrofluorometer (Safire 2, Tecan). To test the activity of compounds against RT, 1 µl of compound in DMSO is added to each well before the addition of RT enzyme solution. Control wells without compound contain the same amount of DMSO. Results are expressed as relative fluorescence i.e. the fluorescence signal of the reaction mix with compound divided by the signal of the same reaction mix without compound.

4. PK Study.

Male Sprague−Dawley rats (180−230 g) were randomly divided into groups (n=3) to receive the low dosage level (5 $mg \cdot kg^{-1}$) or the medium dosage level (10 $mg \cdot kg^{-1}$) of compound. The sample was suspended in a mixture of DMSO, polyethylene glycol (PEG) 400 and normal saline (10/40/50, V/V) before the experiment. Compound was administered to rats by gavage. Blood samples were collected from the sinus jugular into heparinized centrifugation tubes at 5 min, 15 min, 30 min, 1 h, 2 h, 4 h, 6 h, 8 h, 10 h, 12 h, 14 h, and 24 h after dosing. The samples were then centrifuged to separate plasma, which was stored at −80 °C until analysis. LC-MS analysis was used to determine the concentration of compound in plasma. Briefly, 25 µL of plasma was added to 25 µL of internal standard and 200 µL of methanol in a 5 mL centrifugation tube, which was centrifuged at 3000g for 10 min. The supernatant layer was collected, and a 20 µL aliquot was injected for LC-MS analysis. Standard curves in blood were generated by the addition of various concentrations of compound together with internal standard to blank plasma. All samples were quantified with a Shimadzu LC-20AD. The mobile phase was methanol/1.5% acetic acid (50:50, V/V) at a flow rate of 1.0 mL/min, and the test wavelength was 225 nm. All blood samples were centrifuged in an Eppendorf 5430R centrifuge and quantified by Shimadzu LC-20AD. PK status was calculated with WinNonlin 6.3 software using the NCA model.

5. Acute Toxicity Experiment.

Six male Sprague−Dawley rats (252−270 g) were randomly divided into two groups. Rats were fasting for 8 h before administered intragastrically. Then the two groups of rats were subjected to a dose of 183 and 293 $mg \cdot kg^{-1}$ of **12d** and **12z**, respectively.

6. Molecular Modelling

The modeling study was carried out using Schrödinger Maestro 11.4. HIV-1 RT (PDB entry: 2ZD1) is mutated and minimized by Schrödinger BioLuminate. The protein preparation followed a standard protocol.[69, 70] The docking study was performed using Glide. The parameters choose the default without any constraints. MD simulations were carried out for RT in complex with the structurally solved inhibitors. Each system was solvated in a cubic box with explicit TIP3P water and counter ions consisting of a 10Å solvent buffer region from the edge of the complex. The long range electrostatic interactions were evaluated by the Particle-Mesh Ewald method under the periodic boundary condition. 3 ns simulation was carried out for each docked model using Desmond[71-73] with OPLS-AA 2005 force field under the isobaric isothermal (NPT) condition at 300K and 1 atm. The stability of the simulation was assessed by monitoring the RMSD with respect to the minimized starting structure. The molecular docking result was generated using PyMol (http://pymol.sourceforge.net/).

ASSOCIATED CONTENT

Supporting Information is available free of charge on the ACS Publications website at DOI: ###. ^{1}H and ^{13}C NMR spectra, HRMS spectra, and HPLC chromatograms showing the purity of the target compounds (DOCX); SMILES molecular formula strings (CSV).

Notes

The authors declare no competing financial interest.

ACKNOWLEDGMENT

This research was financially supported by National Natural Science Foundation of P. R. China (21372050), Shanghai Municipal Natural Science Foundation (13ZR1402200) and the Young Elite Scientists Sponsorship Program by the China Association for Science and Technology (2017QNRC061). We thank Ningxia Medical University for providing the sources of molecular modeling. The technical assistance of Mr. Kris Uyttersprot, Mrs. Kristien Erven, and Mrs. Cindy Heens for the HIV experiments and HIV RT polymerase assays is gratefully acknowledged. We also acknowledge Prof. Zhengqiang Wang from University of Minnesota for kindly editing on the manuscript.

ABBREVIATIONS

AIDS, acquired immune deficiency syndrome; DAPY, diarylpyrimidine; HAART, highly active antiretroviral therapy; HIV, human immunodeficiency virus; NRTI, nucleoside reverse transcriptase inhibitor; NNRTI, non-nucleoside reverse transcriptase inhibitor; PK, pharmacokinetics; RT, reverse transcriptase; SAR, structure−activity relationship; SI, selectivity index; WT, wild-type; ETR, etravirine; EFV, efavirenz; FI, fusion inhibitor; INSTI, integrase strand transfer inhibitor; PI, protease inhibitor; RAM, resistance-associated mutation.

REFERENCES

1. WHO website. HIV/AIDS fact sheet. http://www.who.int/en/news-room/fact-sheets/detail/hiv-aids (last accessed July 19, 2018)

2. De Clercq, E. New Anti-HIV Agents in Preclinical or Clinical Development. *Frontiers in Medicinal Chemistry* **2003,** 4, 1-62.

3. Kang, D.; Fang, Z.; Li, Z.; Huang, B.; Zhang, H.; Lu, X.; Xu, H.; Zhou, Z.; Ding, X.; Daelemans, D.; De Clercq, E.; Pannecouque, C.; Zhan, P.; Liu, X. Design, Synthesis, and Evaluation of Thiophene[3,2-d]pyrimidine Derivatives as HIV-1 Non-nucleoside Reverse Transcriptase Inhibitors with Significantly Improved Drug Resistance Profiles. *J Med Chem* **2016,** 59, 7991-8007.

4. Shattock, R. J.; Warren, M.; McCormack, S.; Hankins, C. A. AIDS. Turning the tide against HIV. *Science* **2011,** 333, 42-43.

5. Este, J. A.; Cihlar, T. Current status and challenges of antiretroviral research and therapy. *Antiviral Res* **2010,** 85, 25-33.

6. Zhan, P.; Pannecouque, C.; De Clercq, E.; Liu, X. Anti-HIV Drug Discovery and Development: Current Innovations and Future Trends. *J Med Chem* **2016,** 59, 2849-2878.

7. Namasivayam, V.; Vanangamudi, M.; Kramer, V. G.; Kurup, S.; Zhan, P.; Liu, X.; Kongsted, J.; Byrareddy, S. N. The journey of HIV-1 non-nucleoside reverse transcriptase inhibitors (NNRTIs) from lab to clinic. *J Med Chem* **2018,** 10.1021/acs.jmedchem.8b00843.

8. Adams, J.; Patel, N.; Mankaryous, N.; Tadros, M.; Miller, C. D. Nonnucleoside reverse transcriptase inhibitor resistance and the role of the second-generation agents. *Ann Pharmacother* **2010,** 44, 157-165.

9. Maxim Nawrozkij, M. F., Alexandre S. Yablokov, Alessia Lucidi, Daniela; Tomaselli, A. P., Cristina Panella, Gebremedhin Solomon Hailu, Ivan A.; Kirillov, R. B., Eva Riveira Muñoz, Emmanuele Crespan, Jorge I. Armijos-Rivera,; Roberto Cirilli, R. R., Jose A. Este, Giovanni Maga, Antonello Mai, and Dante Rotili. Effect of α-Methoxy Substitution on the anti-HIV Activity of Dihydropyrimidin-4(3H)-ones. *J Med Chem* **2019,** 62, 2, 604-621.

10. Lai, M. T.; Munshi, V.; Lu, M.; Feng, M.; Hrin-Solt, R.; McKenna, P. M.; Hazuda, D. J.; Miller, M. D. Mechanistic Study of Common Non-Nucleoside Reverse Transcriptase Inhibitor-Resistant Mutations with K103N and Y181C Substitutions. *Viruses* **2016,** 8, E263.

11. Udier-Blagovic, M.; Tirado-Rives, J.; Jorgensen, W. L. Validation of a model for the complex of HIV-1 reverse transcriptase with nonnucleoside inhibitor TMC125. *J Am Chem Soc* **2003,** 125, 6016-6017.

12. Cohen, C. J.; Andrade-Villanueva, J.; Clotet, B.; Fourie, J.; Johnson, M. A.; Ruxrungtham, K.; Wu, H.; Zorrilla, C.; Crauwels, H.; Rimsky, L. T.; Vanveggel, S.; Boven, K.; group, T. s. Rilpivirine versus efavirenz with two background nucleoside or nucleotide reverse transcriptase inhibitors in treatment-naive adults infected with HIV-1 (THRIVE): a phase 3, randomised, non-inferiority trial. *Lancet* **2011,** 378, 229-237.

13. Lindberg, J.; Sigurdsson, S.; Lowgren, S.; Andersson, H. O.; Sahlberg, C.; Noreen, R.; Fridborg, K.; Zhang, H.; Unge, T. Structural basis for the inhibitory efficacy of efavirenz (DMP-266), MSC194 and PNU142721 towards the HIV-1 RT K103N mutant. *Eur J Biochem* **2002,** 269, 1670-1677.

14. Ren, J.; Milton, J.; Weaver, K. L.; Short, S. A.; Stuart, D. I.; Stammers, D. K. Structural basis for the resilience of efavirenz (DMP-266) to drug resistance mutations in HIV-1 reverse transcriptase. *Structure* **2000,** 8, 1089-1094.

15. Lansdon, E. B.; Brendza, K. M.; Hung, M.; Wang, R.; Mukund, S.; Jin, D.; Birkus, G.; Kutty, N.; Liu, X. Crystal structures of HIV-1 reverse transcriptase with etravirine (TMC125) and rilpivirine (TMC278): implications for drug design. *J Med Chem* **2010,** 53, 4295-4299.

16. Das, K.; Clark, A. D., Jr.; Lewi, P. J.; Heeres, J.; De Jonge, M. R.; Koymans, L. M.; Vinkers, H. M.; Daeyaert, F.; Ludovici, D. W.; Kukla, M. J.; De Corte, B.; Kavash, R. W.; Ho, C. Y.; Ye, H.; Lichtenstein, M. A.; Andries, K.; Pauwels, R.; de Bethune, M. P.; Boyer, P. L.; Clark, P.; Hughes, S. H.; Janssen, P. A.; Arnold, E. Roles of conformational and positional adaptability in structure-based design of TMC125-R165335 (etravirine) and related non-nucleoside reverse transcriptase inhibitors that are highly potent and effective against wild-type and drug-resistant HIV-1 variants. *J Med Chem* **2004,** 47, 2550-2560.

17. Ludovici, D. W.; De Corte, B. L.; Kukla, M. J.; Ye, H.; Ho, C. Y.; Lichtenstein, M. A.; Kavash, R. W.; Andries, K.; de Bethune, M. P.; Azijn, H.; Pauwels, R.; Lewi, P. J.; Heeres, J.; Koymans, L. M.; de Jonge, M. R.; Van Aken, K. J.; Daeyaert, F. F.; Das, K.; Arnold, E.; Janssen, P. A. Evolution of anti-HIV drug candidates. Part 3: Diarylpyrimidine (DAPY) analogues. *Bioorg Med Chem Lett* **2001,** 11, 2235-2239.

18. Pungpo, P.; Punkvang, A.; Saparpakorn, P.; Wolschann, P.; Hannongbua, S. Recent Advances in NNRTI Design: Computer-Aided Molecular Design Approaches. *Current Computer Aided-Drug Design* **2009,** 5, 174-199.

19. Rotili, D.; Tarantino, D.; Artico, M.; Nawrozkij, M. B.; Gonzalez-Ortega, E.; Clotet, B.; Samuele, A.; Este, J. A.; Maga, G.; Mai, A. Diarylpyrimidine-dihydrobenzyloxopyrimidine hybrids: new, wide-spectrum anti-HIV-1 agents active at (sub)-nanomolar level. *J Med Chem* **2011,** 54, 3091-3096.

20. Xu, H. T.; Colby-Germinario, S. P.; Asahchop, E. L.; Oliveira, M.; McCallum, M.; Schader, S. M.; Han, Y.; Quan, Y.; Sarafianos, S. G.; Wainberg, M. A. Effect of mutations at position E138 in HIV-1 reverse transcriptase and their interactions with the M184I mutation on defining patterns of resistance to nonnucleoside reverse transcriptase inhibitors rilpivirine and etravirine. *Antimicrob Agents Chemother* **2013,** 57, 3100-3109.

21. Asahchop, E. L.; Oliveira, M.; Wainberg, M. A.; Brenner, B. G.; Moisi, D.; Toni, T.; Tremblay, C. L. Characterization of the E138K resistance mutation in HIV-1 reverse transcriptase conferring susceptibility to etravirine in B and non-B HIV-1 subtypes. *Antimicrob Agents Chemother* **2011,** 55, 600-607.

22. Liu, N.; Wei, L.; Huang, L.; Yu, F.; Zheng, W.; Qin, B.; Zhu, D. Q.; Morris-Natschke, S. L.; Jiang, S.; Chen, C. H.; Lee, K. H.; Xie, L. Novel HIV-1 Non-nucleoside Reverse Transcriptase Inhibitor Agents: Optimization of Diarylanilines with High Potency against Wild-Type and Rilpivirine-Resistant E138K Mutant Virus. *J Med Chem* **2016,** 59, 3689-3704.

23. McCallum, M.; Oliveira, M.; Ibanescu, R. I.; Kramer, V. G.; Moisi, D.; Asahchop, E. L.; Brenner, B. G.; Harrigan, P. R.; Xu, H.; Wainberg, M. A. Basis for early and preferential selection of the E138K mutation in HIV-1 reverse transcriptase. *Antimicrob Agents Chemother* **2013,** 57, 4681-4688.

24. Tian, Y.; Liu, Z.; Liu, J.; Huang, B.; Kang, D.; Zhang, H.; De Clercq, E.; Daelemans, D.; Pannecouque, C.; Lee, K. H.; Chen, C. H.; Zhan, P.; Liu, X. Targeting the entrance channel of NNIBP: Discovery of diarylnicotinamide 1,4-disubstituted 1,2,3-triazoles as novel HIV-1 NNRTIs with high potency against wild-type and E138K mutant virus. *Eur J Med Chem* **2018,** 151, 339-350.

25. Kang, D.; Zhang, H.; Wang, Z.; Zhao, T.; Ginex, T.; Luque, F. J.; Yang, Y.; Wu, G.; Feng, D.; Wei, F.; Zhang, J.; De Clercq, E.; Pannecouque, C.; Chen, C. H.; Lee, K. H.; Murugan, N. A.; Steitz, T. A.; Zhan, P.; Liu, X. Identification of Dihydrofuro[3,4- d]pyrimidine Derivatives as Novel HIV-1 Non-Nucleoside Reverse Transcriptase Inhibitors with Promising Antiviral Activities and Desirable Physicochemical Properties. *J Med Chem* **2019,** 62, 1484-1501.

26. Yang, Y.; Kang, D.; Nguyen, L. A.; Smithline, Z. B.; Pannecouque, C.; Zhan, P.; Liu, X.; Steitz, T. A. Structural basis for potent and broad inhibition of HIV-1 RT by thiophene[3,2-d]pyrimidine non-nucleoside inhibitors. *Elife* **2018,** 7, E36340.

27. Frenkel, Y. V.; Clark, A. D., Jr.; Das, K.; Wang, Y. H.; Lewi, P. J.; Janssen, P. A.; Arnold, E. Concentration and pH dependent aggregation of hydrophobic drug molecules and relevance to oral bioavailability. *J Med Chem* **2005,** 48, 1974-1983.

28. Crauwels, H. M.; van Heeswijk, R. P.; Buelens, A.; Stevens, M.; Boven, K.; Hoetelmans, R. M. Impact of food and different meal types on the pharmacokinetics of rilpivirine. *J Clin Pharmacol* **2013,** 53, 834-840.

29. Kakuda, T. N.; Scholler-Gyure, M.; Workman, C.; Arasteh, K.; Pozniak, A. L.; De Smedt, G.; Beets, G.; Peeters, M.; Vandermeulen, K.; Woodfall, B. J.; Hoetelmans, R. M. Single- and multiple-dose pharmacokinetics of etravirine administered as two different formulations in HIV-1-infected patients. *Antivir Ther* **2008,** 13, 655-661.

30. European Medicines Agency web site. Intelence : European public assessment report - Product Information https://www.ema.europa.eu/en/medicines/human/EPAR/intelence (Last updated August 18,2017), https://www.ema.europa.eu/en/medicines/human/EPAR/intelence (Last updated August 18,2017).

31. Huang, B.; Chen, W.; Zhao, T.; Li, Z.; Jiang, X.; Ginex, T.; Vilchez, D.; Luque, F. J.; Kang, D.; Gao, P.; Zhang, J.; Tian, Y.; Daelemans, D.; De Clercq, E.; Pannecouque, C.; Zhan, P.; Liu, X. Exploiting the Tolerant Region I of the Non-Nucleoside Reverse Transcriptase Inhibitor (NNRTI) Binding Pocket: Discovery of Potent Diarylpyrimidine-Typed HIV-1 NNRTIs against Wild-Type and E138K Mutant Virus with Significantly Improved Water Solubility and Favorable Safety Profiles. *J Med Chem* **2019,** 62, 2083-2098.

32. Liang, D. Oral Liquid Formulation of Etravirine for Enhanced Bioavailability. *Journal of Bioequivalence & Bioavailability* **2014,** 06, 46-52.

33. Zeng, Z. S.; He, Q. Q.; Liang, Y. H.; Feng, X. Q.; Chen, F. E.; De Clercq, E.; Balzarini, J.; Pannecouque, C. Hybrid diarylbenzopyrimidine non-nucleoside reverse transcriptase inhibitors as promising new leads for improved anti-HIV-1 chemotherapy. *Bioorg Med Chem* **2010,** 18, 5039-5047.

34. Brown, D. G.; Schauer, P. A.; Borau-Garcia, J.; Fancy, B. R.; Berlinguette, C. P. Stabilization of ruthenium sensitizers to TiO2 surfaces through cooperative anchoring groups. *J Am Chem Soc* **2013,** 135, 1692-1695.

35. Degnan, A. P.; Chaturvedula, P. V.; Conway, C. M.; Cook, D. A.; Davis, C. D.; Denton, R.; Han, X.; Macci, R.; Mathias, N. R.; Moench, P.; Pin, S. S.; Ren, S. X.; Schartman, R.; Signor, L. J.; Thalody, G.; Widmann, K. A.; Xu, C.; Macor, J. E.; Dubowchik, G. M. Discovery of (R)-4-(8-fluoro-2-oxo-1,2-dihydroquinazolin-3(4H)-yl)-N-(3-(7-methyl-1H-indazol-5 -yl)-1-oxo-1-(4-(piperidin-1-yl)piperidin-1-yl)propan-2-yl)piperidine-1-carboxami de (BMS-694153): a potent antagonist of the human calcitonin gene-related peptide receptor for migraine with rapid and efficient intranasal exposure. *J Med Chem* **2008,** 51, 4858-4861.

36. D'Souza, B. R.; Lane, T. K.; Louie, J. Iron-catalyzed cycloaddition of alkynenitriles and alkynes. *Org Lett* **2011,** 13, 2936-2939.

37. Schils, D.; Stappers, F.; Solberghe, G.; van Heck, R.; Coppens, M.; Van den Heuvel, D.; Van der Donck, P.; Callewaert, T.; Meeussen, F.; Bie, E. D.; Eersels, K.; Schouteden, E. Ligandless Heck Coupling between a Halogenated Aniline and Acrylonitrile Catalyzed by Pd/C: Development and Optimization of an Industrial-Scale Heck Process for the Production of a Pharmaceutical Intermediate. *Org Process Res Dev* **2008,** 12, 530-536.

38. Sergeyev, S.; Yadav, A. K.; Franck, P.; Michiels, J.; Lewi, P.; Heeres, J.; Vanham, G.; Arien, K. K.; Vande Velde, C. M.; De Winter, H.; Maes, B. U. 2,6-Di(arylamino)-3-fluoropyridine Derivatives as HIV Non-Nucleoside Reverse Transcriptase Inhibitors. *J Med Chem* **2016,** 59, 1854-1868.

39. Li, Z. L.; Li, J. L.; Liu, J. H.; Zhao, Z. L.; Xia, C. G.; Li, F. W. Palladium Nanoparticles Supported on Nitrogen-Functionalized Active Carbon: A Stable and Highly Efficient Catalyst for the Selective Hydrogenation of Nitroarenes. *Chemcatchem* **2014,** 6, 1333-1339.

40. Sun, Z.; Wang, H.; Wen, K.; Li, Y.; Fan, E. Solvent-free or low-solvent large-scale preparation of chloropyrimidine and analogues. *J Org Chem* **2011,** 76, 4149-4153.

41. Pratap, R.; Parrish, D.; Gunda, P.; Venkataraman, D.; Lakshman, M. K. Influence of biaryl phosphine structure on C-N and C-C bond formation. *J Am Chem Soc* **2009,** 131, 12240-12249.

42. Gunda, P.; Russon, L. M.; Lakshman, M. K. Pd-catalyzed amination of nucleoside arylsulfonates to yield N6-aryl-2,6-diaminopurine nucleosides. *Angew Chem Int Ed Engl* **2004,** 43, 6372-6377.

43. Chou, T. F.; Li, K.; Frankowski, K. J.; Schoenen, F. J.; Deshaies, R. J. Structure-activity relationship study reveals ML240 and ML241 as potent and selective inhibitors of p97 ATPase. *ChemMedChem* **2013,** 8, 297-312.

44. Jiang, N.; Zhai, X.; Zhao, Y.; Liu, Y.; Qi, B.; Tao, H.; Gong, P. Synthesis and biological evaluation of novel 2-(2-arylmethylene)hydrazinyl-4-aminoquinazoline derivatives as potent antitumor agents. *Eur J Med Chem* **2012,** 54, 534-541.

45. Smits, R. A.; de Esch, I. J.; Zuiderveld, O. P.; Broeker, J.; Sansuk, K.; Guaita, E.; Coruzzi, G.; Adami, M.; Haaksma, E.; Leurs, R. Discovery of quinazolines as histamine H4 receptor inverse agonists using a scaffold hopping approach. *J Med Chem* **2008,** 51, 7855-7865.

46. Yoo, E.; Salunke, D. B.; Sil, D.; Guo, X.; Salyer, A. C.; Hermanson, A. R.; Kumar, M.; Malladi, S. S.; Balakrishna, R.; Thompson, W. H.; Tanji, H.; Ohto, U.; Shimizu, T.; David, S. A. Determinants of activity at human Toll-like receptors 7 and 8: quantitative structure-activity relationship (QSAR) of diverse heterocyclic scaffolds. *J Med Chem* **2014,** 57, 7955-7970.

47. Ife, R. J.; Brown, T. H.; Blurton, P.; Keeling, D. J.; Leach, C. A.; Meeson, M. L.; Parsons, M. E.; Theobald, C. J. Reversible inhibitors of the gastric (H+/K+)-ATPase. 5. Substituted 2,4-diaminoquinazolines and thienopyrimidines. *J Med Chem* **1995,** 38, 2763-2773.

48. Chao, Q.; Deng, L.; Shih, H.; Leoni, L. M.; Genini, D.; Carson, D. A.; Cottam, H. B. Substituted isoquinolines and quinazolines as potential antiinflammatory agents. Synthesis and biological evaluation of inhibitors of tumor necrosis factor alpha. *J Med Chem* **1999,** 42, 3860-3873.

49. Gillis, E. P.; Eastman, K. J.; Hill, M. D.; Donnelly, D. J.; Meanwell, N. A. Applications of Fluorine in Medicinal Chemistry. *J Med Chem* **2015,** 58, 8315-8359.

50. Nepali, K.; Lee, H. Y.; Liou, J. P. Nitro-Group-Containing Drugs. *J Med Chem* **2019,** 62, 6, 2851-2893.

51. Krapf, M. K.; Gallus, J.; Namasivayam, V.; Wiese, M. 2,4,6-Substituted Quinazolines with Extraordinary Inhibitory Potency toward ABCG2. *J Med Chem* **2018,** 61, 7952-7976.

52. Krapf, M. K.; Wiese, M. Synthesis and Biological Evaluation of 4-Anilino-quinazolines and -quinolines as Inhibitors of Breast Cancer Resistance Protein (ABCG2). *J Med Chem* **2016,** 59, 5449-5461.

53. Zhou, Z.; Liu, T.; Kang, D.; Huo, Z.; Wu, G.; Daelemans, D.; De Clercq, E.; Pannecouque, C.; Zhan, P.; Liu, X. Discovery of novel diarylpyrimidines as potent HIV-1 NNRTIs by investigating the chemical space of a less explored "hydrophobic channel". *Org Biomol Chem* **2018,** 16, 1014-1028.

54. Houston, J. B. Utility of in vitro drug metabolism data in predicting in vivo metabolic clearance. *Biochem Pharmacol* **1994,** 47, 1469-1479.

55. Young, S. D.; Britcher, S. F.; Tran, L. O.; Payne, L. S.; Lumma, W. C.; Lyle, T. A.; Huff, J. R.; Anderson, P. S.; Olsen, D. B.; Carroll, S. S.; et al. L-743, 726 (DMP-266): a novel, highly potent nonnucleoside inhibitor of the human immunodeficiency virus type 1 reverse transcriptase. *Antimicrob Agents Chemother* **1995,** 39, 2602-2605.

56. Daelemans, D.; Pauwels, R.; De Clercq, E.; Pannecouque, C. A time-of-drug addition approach to target identification of antiviral compounds. *Nat Protoc* **2011,** 6, 925-933.

57. Torres, R. A.; Korzekwa, K. R.; McMasters, D. R.; Fandozzi, C. M.; Jones, J. P. Use of density functional calculations to predict the regioselectivity of drugs and molecules metabolized by aldehyde oxidase. *J Med Chem* **2007,** 50, 4642-4647.

58. Das, K.; Bauman, J. D.; Clark, A. D., Jr.; Frenkel, Y. V.; Lewi, P. J.; Shatkin, A. J.; Hughes, S. H.; Arnold, E. High-resolution structures of HIV-1 reverse transcriptase/TMC278 complexes: strategic flexibility explains potency against resistance mutations. *Proc Natl Acad Sci U S A* **2008,** 105, 1466-1471.

59. La Regina, G.; Coluccia, A.; Silvestri, R. Looking for an active conformation of the future HIV type-1 non-nucleoside reverse transcriptase inhibitors. *Antivir Chem Chemother* **2010,** 20, 213-237.

60. Mirhaji, E.; Yoosefian, M. Structural analysis, solvent effects and intramolecular interactions in rilpivirine: A new non-nucleoside reverse transcriptase inhibitor for HIV treatment. *Journal of Molecular Liquids* **2017,** 246, 124-130.

61. Wetzel, M.; Marchais-Oberwinkler, S.; Perspicace, E.; Moller, G.; Adamski, J.; Hartmann, R. W. Introduction of an electron withdrawing group on the hydroxyphenylnaphthol scaffold improves the potency of 17beta-hydroxysteroid dehydrogenase type 2 (17beta-HSD2) inhibitors. *J Med Chem* **2011,** 54, 7547-7557.

62. Pannecouque, C.; Daelemans, D.; De Clercq, E. Tetrazolium-based colorimetric assay for the detection of HIV replication inhibitors: revisited 20 years later. *Nat Protoc* **2008,** 3, 427-434.

63. Pauwels, R.; Balzarini, J.; Baba, M.; Snoeck, R.; Schols, D.; Herdewijn, P.; Desmyter, J.; De Clercq, E. Rapid and automated tetrazolium-based colorimetric assay for the detection of anti-HIV compounds. *J Virol Methods* **1988,** 20, 309-321.

64. Balzarini, J.; Karlsson, A.; Perez-Perez, M. J.; Vrang, L.; Walbers, J.; Zhang, H.; Oberg, B.; Vandamme, A. M.; Camarasa, M. J.; De Clercq, E. HIV-1-specific reverse transcriptase inhibitors show differential activity against HIV-1 mutant strains containing different amino acid substitutions in the reverse transcriptase. *Virology* **1993,** 192, 246-253.

65. Balzarini, J.; Karlsson, A.; Perez-Perez, M. J.; Camarasa, M. J.; Tarpley, W. G.; De Clercq, E. Treatment of human immunodeficiency virus type 1 (HIV-1)-infected cells with combinations of HIV-1-specific inhibitors results in a different resistance pattern than does treatment with single-drug therapy. *J Virol* **1993,** 67, 5353-5359.

66. Balzarini, J.; Karlsson, A.; Vandamme, A. M.; Perez-Perez, M. J.; Zhang, H.; Vrang, L.; Oberg, B.; Backbro, K.; Unge, T.; San-Felix, A.; et al. Human immunodeficiency virus type 1 (HIV-1) strains selected for resistance against the HIV-1-specific [2',5'-bis-O-(tert-butyldimethylsilyl)-3'-spiro- 5"-(4"-amino-1",2"-oxathiole-2",2"-dioxide)]-beta-D-pentofurano syl (TSAO) nucleoside analogues retain sensitivity to HIV-1-specific nonnucleoside inhibitors. *Proc Natl Acad Sci U S A* **1993,** 90, 6952-6956.

67. Auwerx, J.; North, T. W.; Preston, B. D.; Klarmann, G. J.; De Clercq, E.; Balzarini, J. Chimeric human immunodeficiency virus type 1 and feline immunodeficiency virus reverse transcriptases: role of the subunits in resistance/sensitivity to non-nucleoside reverse transcriptase inhibitors. *Mol Pharmacol* **2002,** 61, 400-406.

68. Singer, V. L.; Jones, L. J.; Yue, S. T.; Haugland, R. P. Characterization of PicoGreen reagent and development of a fluorescence-based solution assay for double-stranded DNA quantitation. *Anal Biochem* **1997,** 249, 228-238.

69. Wang, H.; Wei, W.; Lan, X.; Liu, N.; Li, Y.; Ma, H.; Sun, T.; Peng, X.; Zhuang, C.; Yu, J. Neuroprotective Effect of Swertiamain on Cerebral Ischemia/Reperfusion Injury by Inducing the Nrf2 Protective Pathway. *ACS Chem Neurosci* **2019,** 10, 5, 2276-2286.

70. Zhuang, C.; Narayanapillai, S.; Zhang, W.; Sham, Y. Y.; Xing, C. Rapid identification of Keap1-Nrf2 small-molecule inhibitors through structure-based virtual screening and hit-based substructure search. *J Med Chem* **2014,** 57, 1121-1126.

71. D.E.S. Research, Desmond Molecular Dynamics System for Academic. **2017**.

72. Sang, Y.; Han, S.; Pannecouque, C.; De Clercq, E.; Zhuang, C.; Chen, F. Conformational restriction design of thiophene-biphenyl-DAPY HIV-1 non-nucleoside reverse transcriptase inhibitors. *Eur J Med Chem* **2019,** 182, 111603.

73. Zhuang, C.; Sheng, C.; Shin, W. S.; Wu, Y.; Li, J.; Yao, J.; Dong, G.; Zhang, W.; Sham, Y. Y.; Miao, Z.; Zhang, W. A novel drug discovery strategy: mechanistic investigation of an enantiomeric antitumor agent targeting dual p53 and NF-kappaB pathways. *Oncotarget* **2014,** 5, 10830-10839.

Table of Contents Graphic

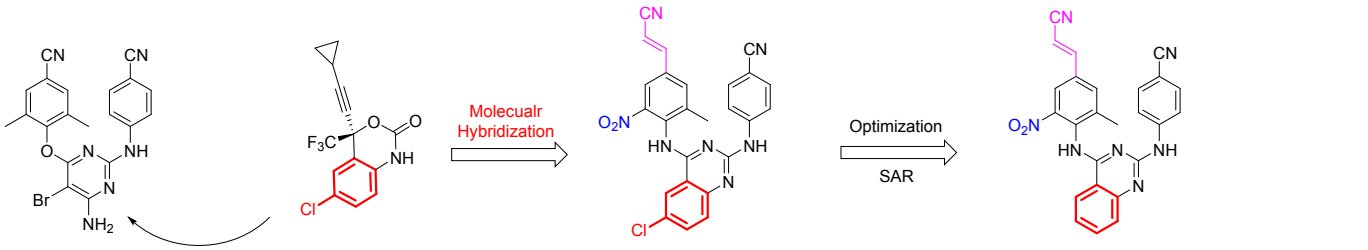

ETR

EC_{50} (nM)= 3.9 ± 1.4 (WT)
10.9 ± 7.4 (E138K)
3.5 ± 0.9 (K103N)
The oral bioavailability is unknown due to its bad solubility.

EFV

3.2 ± 1.6 (WT)
5.4 ± 1.3 (E138K)
147.4 ± 85.9 (K103N)
Rat oral bioavailability (F) = 16%

12d

EC_{50} (nM)= 10.6 ± 10.0 (WT)
17.7 ± 2.7 (E138K)
10.2 ± 0.8 (K103N)
$CL_{int,\ microsome}$ (μL/min/mg) = 30.6 (Rat)
14.4 (Human)
Rat oral bioavailability (F) = 15.5%
SI= 375

12z

EC_{50} (nM)= 3.4 ± 0.9 (WT)
4.3 ± 1.3 (E138K)
3.6 ± 0.9 (K103N)
$CL_{int,\ microsome}$ (μL/min/mg) = 33.2 (Rat)
34.5 (Human)
Rat oral bioavailability (F) = 16.5%
SI= 1827